

Project no.:

608608

Project acronym:

MiReCOL

Project title:

Mitigation and remediation of leakage from geological storage

Collaborative Project

Start date of project: 2014-03-01

Duration: 3 years

D4.3

CO₂ back-production at the Ketzin and K12-B sites

Revision: 1

Organisation name of lead contractor for this deliverable:

GFZ

Project co-funded by the European Commission within the Seventh Framework Programme		
Dissemination Level		
PU	Public	X
PP	Restricted to other programme participants (including the Commission Services)	
RE	Restricted to a group specified by the consortium (including the Commission Services)	
CO	Confidential , only for members of the consortium (including the Commission Services)	

Deliverable number:	D4.3
Deliverable name:	CO ₂ back-production at the Ketzin and K12-B sites
Work package:	WP4 Reservoir pressure management
Lead contractor:	GFZ

Status of deliverable		
Action	By	Date
Submitted (Author(s))	C. Schmidt-Hattenberger, B. Wiese, A. Liebscher, Fabian Möller	05-Mar-2016
Verified (WP-leader)	Cornelia Schmidt-Hattenberger	30-Jun-2016
Approved (SP-leader)	Axel Liebscher	04-Jul-2016

Author(s)		
Name	Organisation	E-mail
Cornelia Schmidt-Hattenberger	GFZ	conny@gfz-potsdam.de
Bernd Wiese	GFZ	wiese@gfz-potsdam.de
Axel Liebscher	GFZ	alieb@gfz-potsdam.de
Fabian Möller	GFZ	fmöller@gfz-potsdam.de
Sevket Durucan	Imperial	s.durucan@imperial.ac.uk
Anna Korre	Imperial	a.korre@imperial.ac.uk
Rajesh Govindan	Imperial	r.govindan07@imperial.ac.uk
Guangyao Si	Imperial	g.si11@imperial.ac.uk
Cor Hofstee	TNO	Cor.Hofstee@tno.nl

Public abstract
<p>This report is part of the research project MiReCOL (Mitigation and Remediation of CO₂ leakage) funded by the EU FP7 programme¹. Research activities aim at developing a handbook of corrective measures that can be considered in the event of undesired migration of CO₂ in the deep subsurface reservoirs. MiReCOL results support CO₂ storage project operators in assessing the value of specific corrective measures if the CO₂ in the storage reservoir does not behave as expected. The report summarizes the studies regarding a "Feasibility test and numerical modelling of CO₂ back-production as remediation measure to reduce reservoir pressure", conducted at the Ketzin CO₂ pilot site, Germany. The report represents a description of the technical operation as well as results of numerical simulations of the pressure evolution and produced CO₂/brine volumes. Conclusions on the deployment of this type of pressure management techniques as corrective measures are drawn. Results from the Ketzin pilot study are compared with those of the K12-B gas field (Dutch North sea sector), a real-production case study where two back-production periods have been investigated.</p>

¹ More information on the MiReCOL project can be found at www.mirecol-CO2.eu.

Inhalt

1	INTRODUCTION	6
2	TECHNICAL IMPLEMENTATION AND MONITORING RESULTS	8
2.1	Organisation of the operation	9
2.2	Technical description of facility	9
2.3	Test procedure	10
2.4	Safety measures	11
2.5	Disposal of co-produced brine.....	11
2.6	Pressure and temperature behaviour.....	11
2.7	Geoelectric measurements.....	13
2.8	Gas analysis	15
2.9	Water analysis.....	16
3	NUMERICAL SIMULATIONS AND RESULTS	18
3.1	Numerical simulations in advance of the field test.....	18
3.2	Numerical simulations after the field test (Imperial).....	19
3.3	Development of an inverse Ketzin model for near-wellbore studies (GFZ)	26
4	PRACTICAL UNDERSTANDING OF WELL LOAD-UP BEHAVIOUR	32
4.1	Well effects during back-production	32
4.2	Turner criterion.....	32
5	CASE STUDY OF THE K12-B GAS FIELD	34
5.1	Field site	34
5.2	Back-production experiments.....	35
5.3	Modelling approach.....	36
5.4	Results	37
5.5	Discussion.....	42
6	SUMMARY	43
7	REFERENCES	44

1 INTRODUCTION

CO₂ migration and leakage through faults, wellbores and non-sealing cap rock have been studied in various simulations by several authors (see for example Celia et al., 2005; Nordbotten et al., 2005; Pruess, 2006; Pruess, 2008; Yamamoto et al., 2009; Birkholzer et al., 2009). Mitigation and remedial measures of these potential undesired migration/leakage scenarios are mainly associated with operational activities, some of which could be implemented immediately, whereas others require more time and technical effort (Manceau et al., 2014).

During regular injection operation, a temporary cease or reduction of injected CO₂ is the most immediate remedial action that can be implemented if a leakage is detected. Reducing the amount of injected gas will lower the rate of pressure increase as potential driving factor causing the undesired migration of CO₂.

In the post-injection phase, a back-production process of formerly injected CO₂ may provide a suitable technique to (i) mitigate undesired migration of CO₂ in the reservoir by inducing a pressure-gradient driven directed flow of CO₂ and (ii) manage the reservoir pressure. Furthermore, the production of CO₂ will also form an integral part of any temporary storage of CO₂ in the frame of a different carbon capture storage & utilisation (James, 2013) and/or power-to-gas concepts (Grond and Holstein, 2014). In CO₂ storage combined with enhanced hydrocarbon recovery CO₂ will be co-produced with the recovered hydrocarbons. The production ratio of gas to reservoir fluid is an important design parameter in all contexts. Below a minimum flow velocity in a well, the critical Turner velocity v_{Tur} , no fluid is produced and well load up (cone shaped brine accumulation) occurs.

To study its general feasibility, a CO₂ back-production experiment was conducted in October 2014 at the Ketzin pilot site, Germany (Martens et al., 2015). Over a two-week period a total amount of 240 tonnes of CO₂ and 55 m³ of brine were safely extracted from the reservoir. Geoelectrical monitoring by means of a permanent electrode array at the production well was capable of tracking the back-production process and the back flow of brine into the parts previously filled with CO₂. Preliminary results also show that the back-produced CO₂ at Ketzin has a purity >97 %. Secondary component in the CO₂ stream is N₂ with <3 %, which probably results from previous field tests. The geochemical results will help to verify laboratory experiments which are typically performed in simplified synthetic systems. Numerical simulations were carried out (i) in advance of the field test to support its design and (ii) after the field test in order to demonstrate the performance of the history-matched model. Considering the effective time schedule and the maximum allowed flow rates, the total amount of back-produced CO₂ was underestimated by about 14 % in the numerical simulations (Martens et al., 2015a).

The results obtained at the Ketzin site refer to the pilot scale field trial. Upscaling of the results to industrial scale is possible and has been underlined by further numerical simulations, but should be first tested and validated at demonstration projects.

The case study of the K12-B gas field in the North Sea demonstrates the injection into a mature gas field as potential option for long-term CO₂ storage. Frequently, the injection process is initially also aimed for enhancing the gas recovery (EGR). The K12-B gas field is one of the first and only gas fields in the Netherlands where injection of CO₂ was carried out. Residual CO₂ from the gas production was re-injected into different compartments of the field during different injection intervals. After the injection periods a number of back-production test have been carried out. These operations are numerically analysed for key factors such as recovery rate, CO₂ ratio, well pressure and water coproduction. In addition, the measured data as well as observations at the field are history matched with a compositional reservoir simulator.

2 TECHNICAL IMPLEMENTATION AND MONITORING RESULTS

The German Research Centre for Geosciences operates the Ketzin CO₂ pilot site, the first European on-shore geological storage experiment in a saline aquifer of the North East German Basin (Liebscher et al., 2013). The active CO₂ injection and storage phase covers the period from June 2008 to August 2013. During this time, a total amount of approximately 67 kt of carbon dioxide (CO₂) was stored in the sandstone layers of the Stuttgart formation (Martens et al., 2015b). In the frame of several Ketzin project phases, the behavior of CO₂ in the storage reservoir and the resulting behavior of the storage complex have been studied by a multi-disciplinary scientific monitoring concept, comprising geophysical and geochemical methods, as well as numerical modelling studies.

To test the general feasibility of storage, including the retrievability of the injected CO₂, a so-called back-production experiment was carried out in October 2014. Along with the technical and operational details, the following questions should be examined:

- Recovery of process parameters (temperature profiles along the production tubing, well-head and bottom-hole pressures, flow rates) to assess the reservoir and wellbore behavior and to evaluate the technical feasibility
- Investigation of the composition of the back-produced CO₂
- Does the gas quality adequately fit into the context of carbon capture storage and utilization (CCSU), i.e. in particular to "power to gas" concepts?
- What quantities of formation water are simultaneously produced and what is the composition?
- What technical and organisational measures have to be taken for a safe back-production operation of CO₂?

The overarching objective of this experiment was evaluating whether this technical operation can be used as a corrective measure for pressure management of a storage reservoir. Among other techniques of pressure regulation and CO₂ plume management, the conversion of an injection well into a producing well for accelerating the pressure reduction may be considered (Manceau et al., 2014). For simplification purposes, one can assume that the well is producing at a constant rate which is equal to the previous injection rate (CO₂ injection rate at Ketzin: ~min 1.6 t/h to max. 3.2 t/h). This corresponds to 0.5 kg/s – 0.8 kg/s and is in the order of magnitude of a standard water pump (~ 1kg/s or 1liter/s). During the CO₂ extraction, pressure in the injection zone declines. When the extraction stops, the pressure field is equilibrated in the reservoir leading to a pressure recovery in the injection zone.

2.1 Organisation of the operation

The CO₂ back-production was conducted from October 15, 2014 until October 27, 2014. GFZ had commissioned the company Weatherford Energy Services for conduction all technical operations. A professional safe guard as well as scientific personnel of GFZ was on site every day.

The test operation at the Ketzin pilot site took place around the clock seven days a week. A corresponding exemption according the German law (ArbZG) was submitted together with the technical procedures and received approval from the Mining Authority of the Federal State of Brandenburg. In order to estimate a possible noise pollution of the neighborhood by the CO₂ back-production, an acoustic certificate was conducted by an engineering bureau on October 15, 2014, during the peak hours from 10:00 am to 4:00 pm. In this period, all intended production rates were tested. The result showed that the CO₂ back-production does not cause any harmful effects by noise pollution.

2.2 Technical description of facility

Weatherford Energy Services provided the technical equipment for conducting the back-production test (Figure 1), as well as the skilled engineering personnel for the operation.

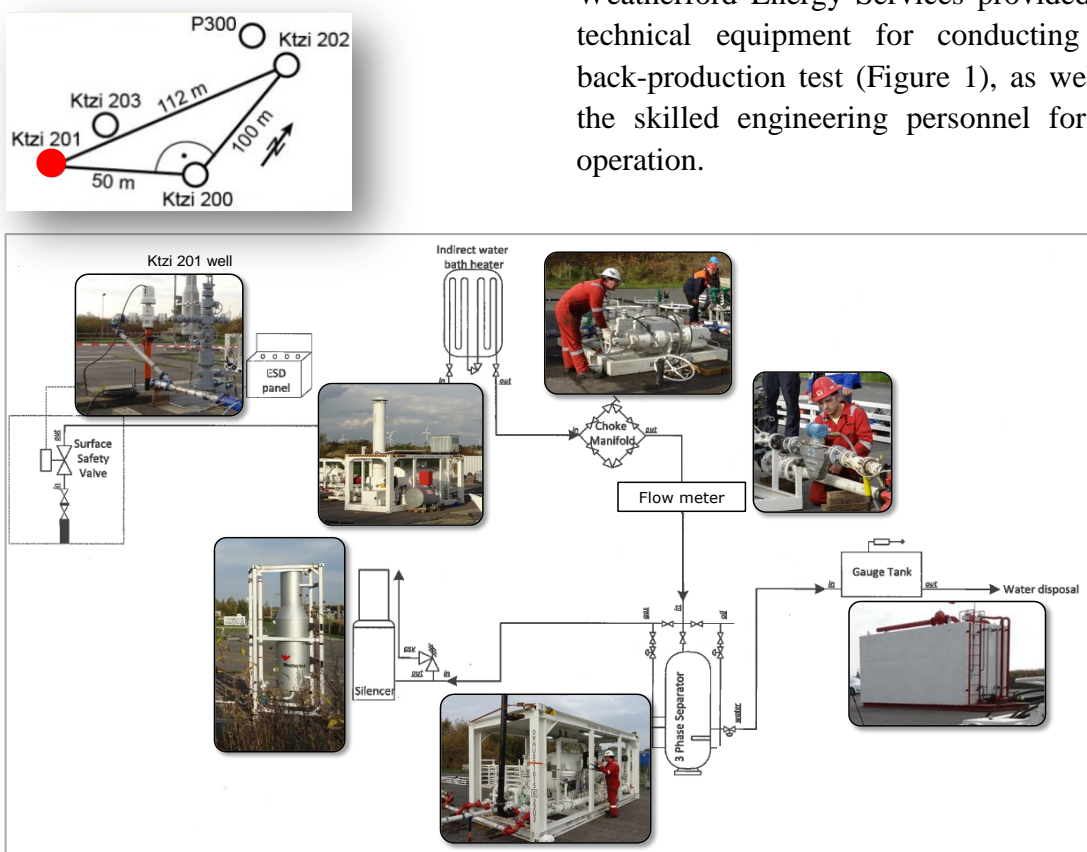


Figure 1: Technical components for the back-production test (Martens et al., 2015). In the schematic borehole layout (top left), the well Ktzi 201 is marked by a red dot. The CO₂ was flowing at the wellhead of Ktzi 201 through a surface safety valve (Figure 1).

Thereafter, it was heated by means of a diesel-powered waterbath-heater to about 50 °C to prevent dry ice formation. After preheating, a manual volume control was carried out by means of a choke manifold. Co-produced brine from the reservoir was separated in a separator, stacked in a tank on site and properly disposed (see also section 2.4). The CO₂ was vented via a silenced 6 m high stack system in the ambient air. Gas and water samples for further investigation were taken at the separator (see sections 3.3 and 3.4).

2.3 Test procedure

On October 15, 2014 at 10:50 am, extraction rates of about 900 kg/h, 2.000 kg/h and 3.500 kg/h were conducted for at least one hour each, in order to demonstrate the general feasibility and to carry out a meaningful measurement of the noise level (see section 2.1). The operational protocol is presented in Table 1.

Table 1: Operational protocol during the back-production experiment.

Start time	End time	Rate
15.10.2014 (4:00 pm)	20.10.2014 (12:00 am)	continuously, about 800 kg/h
20.10.2014 (12:00 am)	22.10.2014 (5:00 pm)	continuously, ca. 1.600 kg/h
23.10.2014 (11:00 am)	27.10.2014 (8:00 pm)	alternating regime with a mean flow rate of 800 kg/h during day shift (8:00 am - 8:00 pm); and switch off during night shift (8:00 pm – 8:00 am)

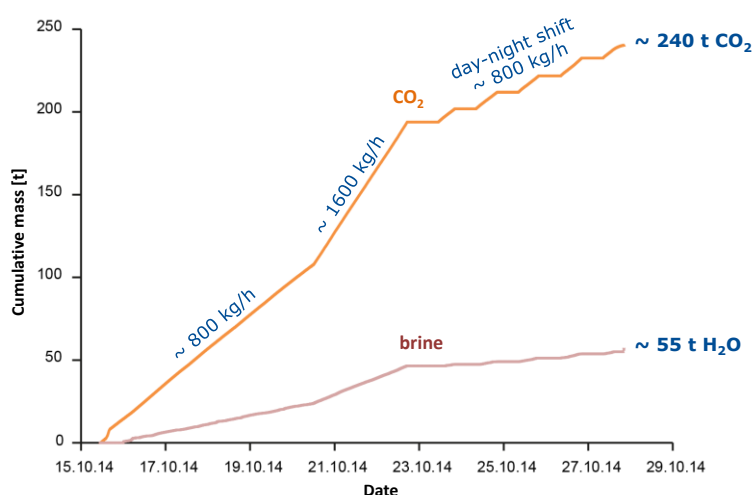


Figure 2: Cumulative mass of produced CO₂ and brine, with various rates during a period of two weeks.

Before the experiment ended, the rates were successively decreased every hour by 100 kg/h, starting from 800 kg/h towards 200 kg/h, in order to determine the final rate of co-produced formation water. This was the case at a rate of 500 kg/h. The experiment was terminated on 27.10.2014 at 8:00 pm. The total amount of produced CO₂ and brine is presented in Figure 2.

2.4 Safety measures

Before starting the experiment, a safety-training meeting with all personnel involved was conducted. Major objective of this instruction was the fulfilling of the establishment order. Particular working conditions have been discussed and appointed. A locked security zone (about 28 m x 35 m) around the stack system was set up as safety measure against possible increased CO₂ concentrations in the ambient air. In addition, the duration of stay for the staff in the environment of facility components (choke manifold, separator, etc.) has been limited to a minimum to control and monitor the experiment. For permanent CO₂ concentration measurements within the safety zone of the technical facility, the field crew used a typical handheld instrument. After October 16, the CO₂ concentrations outside of the safety zone were recorded by Weatherford or GFZ, measured at least every four hours with the same instrument. A total of 72 measurement patrols were carried out. For the majority of measurements (57 of 72) CO₂ concentrations <0.5% by volume, usually in the range of 0.04 vol% (in ambient air), have been recorded. It was also found that CO₂ concentrations show temporarily - highly dependent on wind conditions – a local increase (> 0.50 vol .-%). In the case of 5 measurement patrols local CO₂ concentrations > 1% by volume were recorded due to very calm weather conditions. 1% by volume represents the critical short-term exposure value for CO₂ (acc. To TRGS 900, Class II, overload factor 2). To take into account of the strict health and safety regulations, the back-production rate was reduced to 800 kg /hours after October 23, 2014 and the operation was carried out only during the day shift. From October 20, 2014, two additional mobile fan systems were made available and have been used in the work area for a more rapid mixing of the CO₂ with the ambient air.

2.5 Disposal of co-produced brine

A total amount of 61.74 tonnes of co-produced brine with a high salinity (see subsection 2.9) had to be disposed. This was carried out by a commissioned company. In addition, measurement of radioactivity of each fetched batch of formation water has been conducted. No radioactivity has been detected. Also, the final measurement of all technical system components by Weatherford revealed no radioactive contamination.

2.6 Pressure and temperature behaviour

For the whole test period, besides the continuous measurement of CO₂ and brine production rates, well-head and bottom-hole pressure at Ktzi 201 was recorded (Figure 3). After adjusting a continuous production rate the pressure sensor of the well Ktzi 201

at 550 m depth displayed a dynamic equilibrium pressure of approximately 61 bar from October 16, 2014, and a dynamic equilibrium pressure of around 46 bar at the wellhead since October 18, 2014, . The dynamic equilibrium was not significantly disturbed by doubling the production rate at 1,600 kg/h on October 20, 2014. After October 23, 2014, when the alternating regime of 12 hours production at a rate of 800 kg/h with subsequent shutting off the wellbore for another 12 hours was introduced, a very rapid adjustment of the pressure to the level before the start of back-production (~ 65 bar) was observed. The pressure readings during the continuous production operation were comparable at ~ 61 bar.

The very short periodic pressure drops (daily at 5:20 am) were caused by technical reasons. The data acquisition system has been re-started automatically on a daily basis during the night-time in order to increase the stability of the measurements.

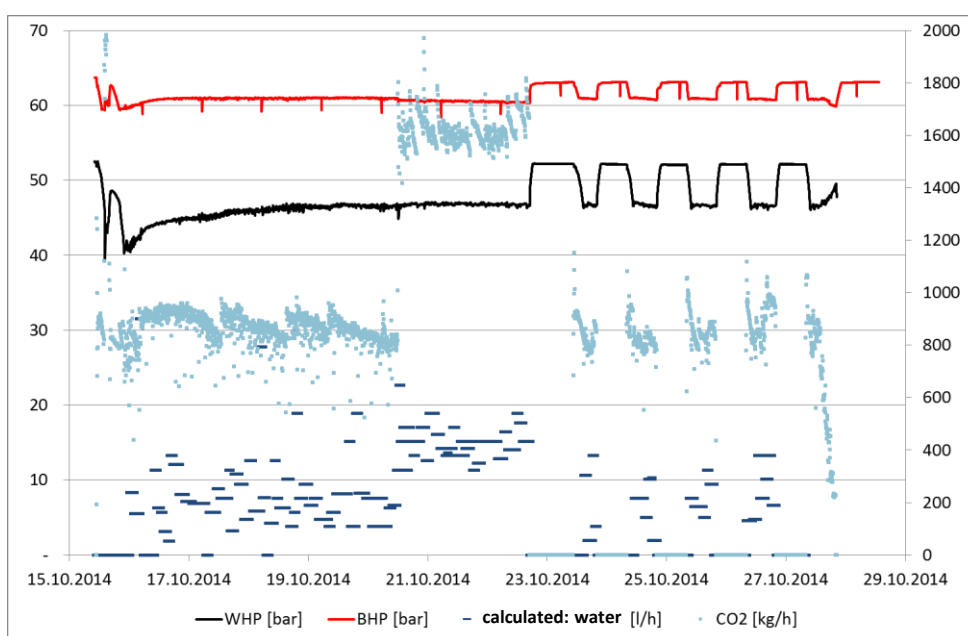


Figure 3: Overview of the measured parameters during the CO₂ back-production experiments at Ktzi 201: WHP (wellhead pressure), BHP (bottomhole pressure) @ 550 m depth. Formation water has been co-produced until a rate of 500 kg/h CO₂.

Figure 4 displays temperature profiles, continuously recorded by a distributed temperature sensing (DTS) system at the fibre-optic cables along the 3.5" production tubing of Ktzi 201. The baseline measurement (red curve) was recorded before the start of back-production and represents the temperature profile of the stagnant wellbore. It shows the continuous re-allocation of CO₂ with condensation in the upper region and evaporation in the lower area of the wellbore, known as heat pipe effect. After starting the back-production, a linear temperature profile (different colored curves of Figure 4)

occurs, presenting gaseous CO₂ in the entire well. This condition was observed during the entire back-production process.

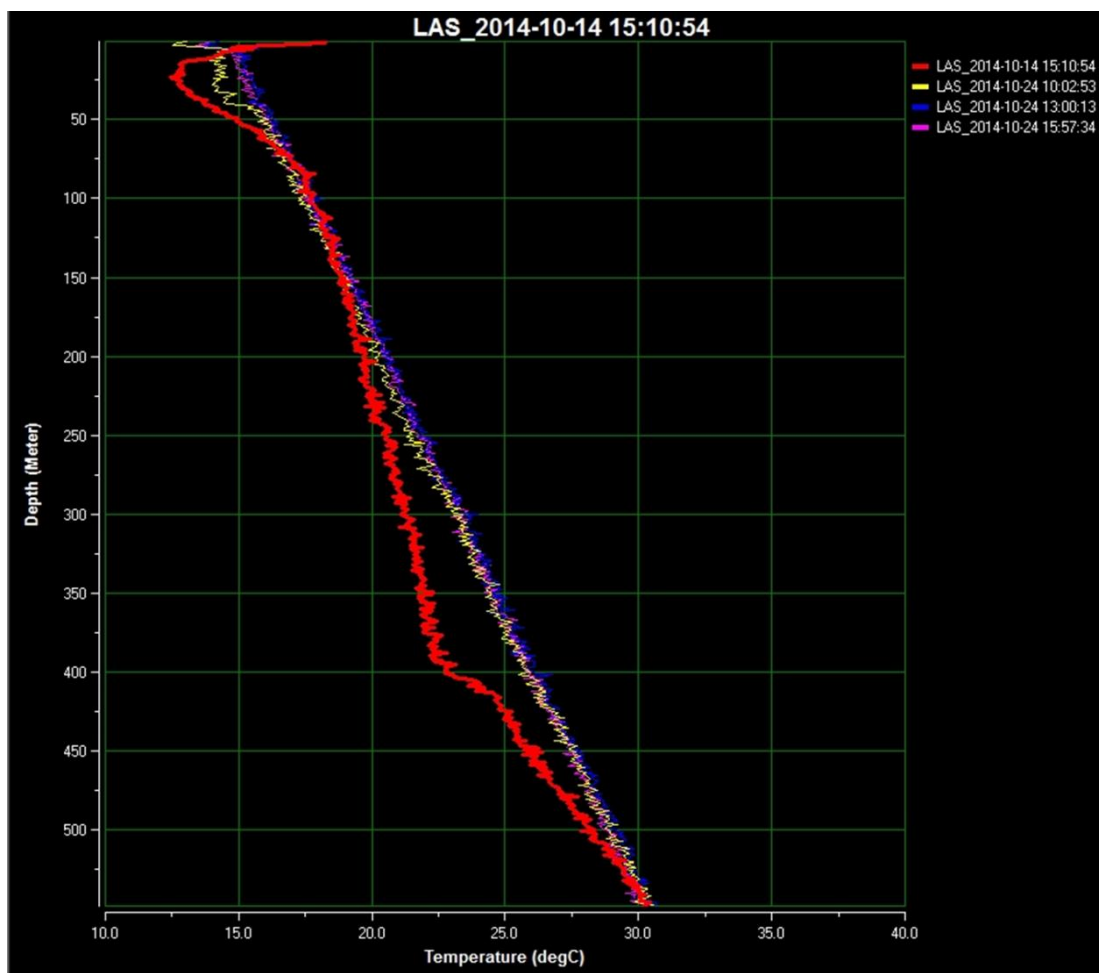


Figure 4: Temperature profiles of production well Ktzi 201 during the back-production experiment. Baseline (14.10.2014/red curve) and three different measurements (various times at 24.10.2014).

2.7 Geoelectric measurements

The back-production test has been accompanied by regular geoelectrical measurements based on the permanent downhole electrodes of the crosshole plane Ktzi 201-Ktzi 200 (Martens et al., 2015). Daily recordings have been carried out but some data was lost due to remote-control interruption. A direct indication of the near-wellbore processes during the back-production experiment is given by the contact resistances, which represent raw data of the electrode array. The data describe the coupling behavior of the electrodes with the surrounding rock mass, and image the contact with high-conductive brine or high-resistant CO₂. Usually, the electrodes are grouted by cement and provide stable contact resistance values during all measurement phases. In case of the

injection/production well Ktzi 201, a partially open annular space exists where fluid exchange between brine and CO₂ occurs. Therefore, the contact resistances directly indicate the type of fluid in the borehole.

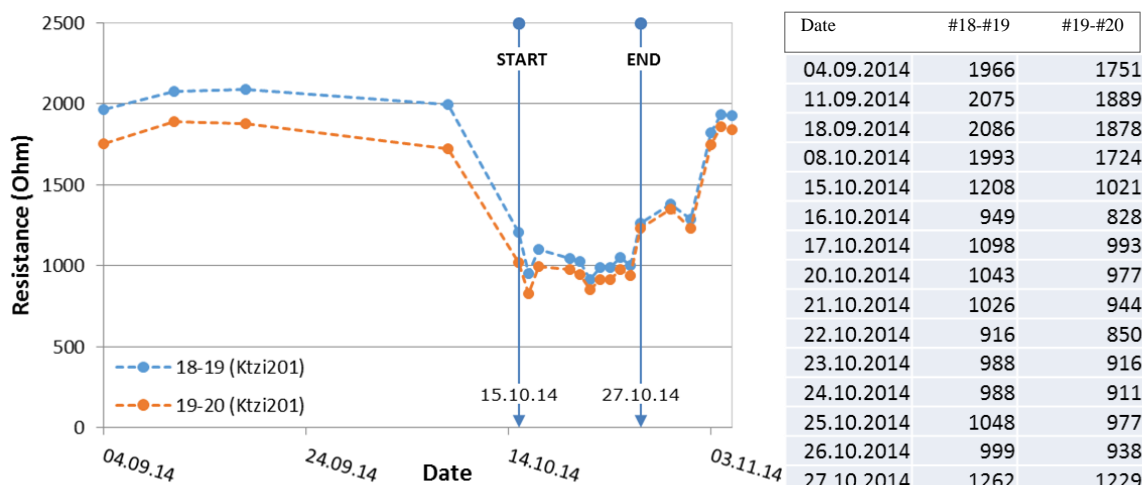


Figure 5: Display of contact resistance values measured at the permanent downhole electrodes #18-#19 and #19-#20 at the Ktzi 201 well, recorded from Sep-04 until Oct-27, 2014. The time window of Oct 15th until Oct 27th, 2014 indicates the back-production process, where the variations of the contact resistances correlate with the pressure fluctuations (measured as BHP @ 550 m). Data loss took place between Oct-18/Oct-19, 2014.

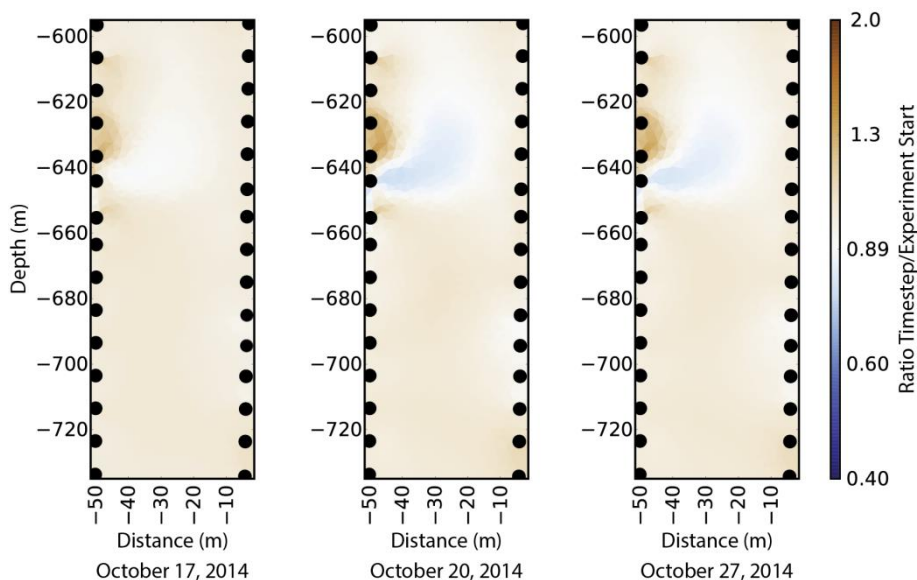


Figure 6: Tomographic results show the baseline (1) and two following time steps (2, 3), where stimulation of formation water (blue colored) is seen together with the ascending CO₂ (brown colored).

As seen in Figure 5, the observed electrodes start with high resistance values which indicates CO₂ in the annulus, equilibrated during the previous post-injection phase. The back-production causes a significant decrease in the resistance values due to ascending brine, which occurs together with the vented CO₂. This behavior can also be demonstrated by the tomographic results of Figure 6, where a comparison between the baseline situation (October 14, 2014) and various time-steps from the back-production phase is given.

2.8 Gas analysis

To determine the composition of the back-produced gas, a special pipe from the separator gas outlet to the analyser in the scientific cabin has been installed. For continuous gas analysis, a mass spectrometer, a gas chromatograph and a photoacoustic sensor were used. Every day, gas sample tubes were repeatedly filled for a subsequent study of stable carbon isotopes in the laboratory.

The extracted gas consisted of > 97% of CO₂ (Figure 7). The second most component was nitrogen, the concentration of which continuously decreased towards October 23, 2014 (3 to 1.4%), the beginning of the alternating load regime. During the day shift a mixture of ~ 98.5/~ 1.5% CO₂/N₂ were recorded, with slightly increased nitrogen levels in the morning after the re-start.

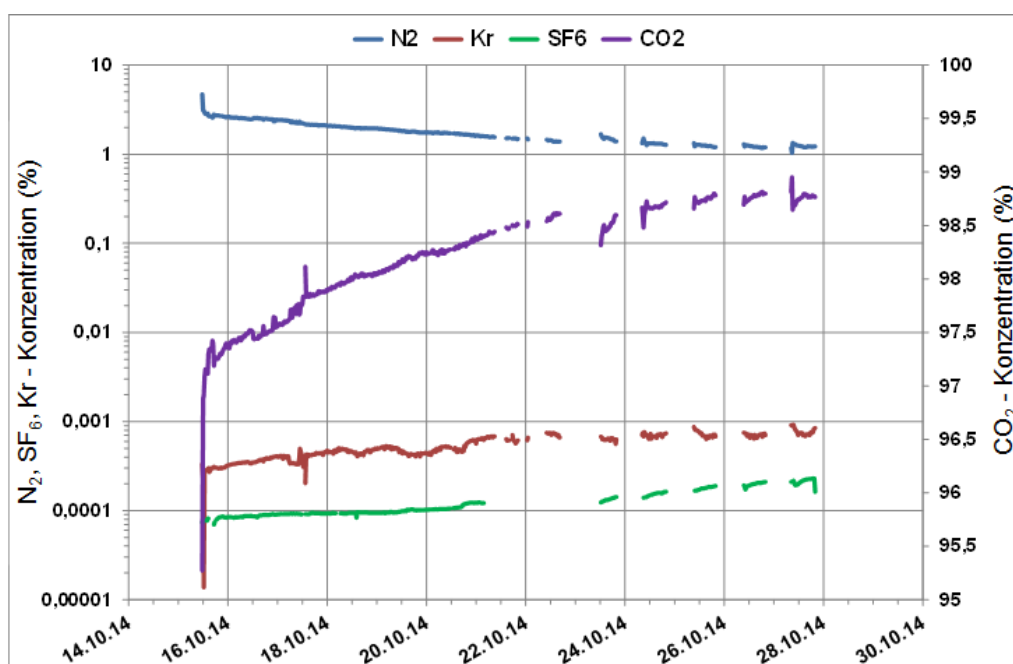


Figure 7: Composition of the back-produced gas.

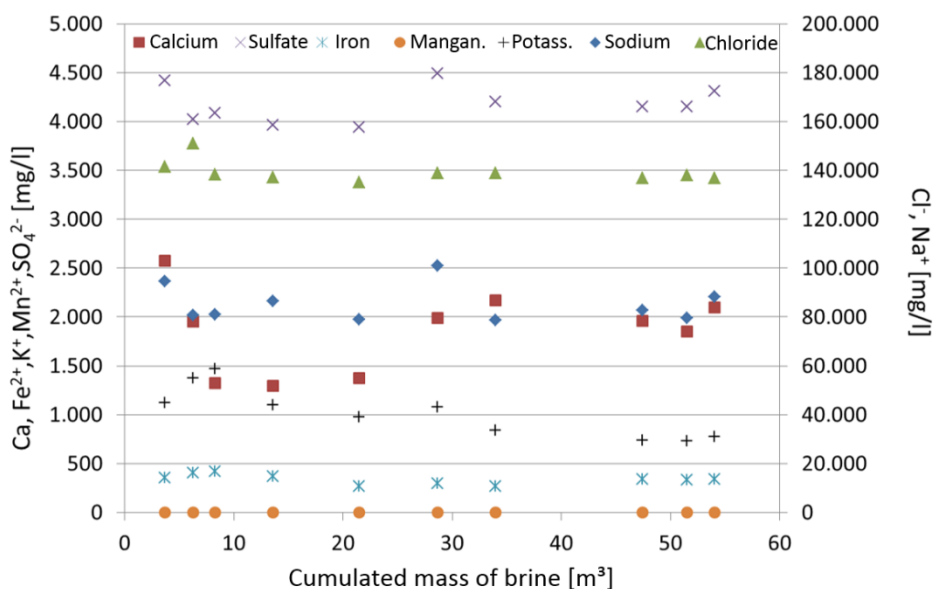
Furthermore, small amounts of methane, carbon monoxide and hydrogen (<0.01%) as well as krypton and sulfur hexafluoride (concentrations <0.001%, e.g., used in 2013 as a gaseous tracer during the injection) were measured.

It is known from gas measurements on fluids of Ktzi 200 before the start of injection that the original pore fluid (L_{Gas}/L_{Fluid} : 0,017) contains methane, CO₂, H₂ and N₂ (0.17 / 0.08 / 0.14 / 17.9 mg/l). After the arrival of CO₂ at Ktzi 200 increased concentrations of methane and hydrogen (1.44 & 0.43 mg/l) were measured. Nitrogen was also detected, although at low concentrations (1.48 mg/l). In particular, the nitrogen can thus originate from either the injection operation or the CO₂-N₂ co-injection test in 2013, and/or from the original pore fluid. Investigations on the isotopic composition are still in progress. To answer the question, whether the composition of the produced gas will allow application of carbon capture, storage and usage (CCSU), gas samples were provided to the Brandenburg Technical University Cottbus (BTU). In cooperation between GFZ and BTU, catalytically guided methanation of CO₂ samples from Ketzin is under investigation. The results are also currently pending.

2.9 Water analysis

Water samples at the separator were taken to study the chemical composition of the entrained water from the Ktzi 201 during the back-production process. The electrical conductivity of the samples was in the range 206 to 225 mS/cm. The pH ranged from 5.7 to 6.0.

Figure 8: Analysis of water samples taken at the separator during the back-production process.



In addition, 10 samples were analysed by the Potsdam Water and Environmental Laboratory regarding inorganic parameters and selected heavy metals (iron, manganese).

Figure 8 shows the results of the water sample analysis based on the cumulative mass of brine. In the 10 samples, stable values of analysed parameters versus cumulative amount of brine are shown. Over the test period, no substantial changes were determined in the water composition.

In particular, the measured values for chloride, sulfate, sodium and the electrical conductivity show that the produced water represents highly concentrated salt water. Concentrations remain comparatively constant during the experiment. Nevertheless, some variations in Calcium and Sulphate may indicate geochemical processes. There is a certain decrease of the Iron concentration, although a little bit masked by the axis scale. This is partially attributed to borehole corrosion. Compared to pre-injection conditions, the Iron concentrations in the reservoir are increased by more than factor 2. Since this increase is comparatively constant and does not have a strong correlation to the borehole, it is considered to be the result of geochemical reactions of pyrite or iron-oxides.

3 NUMERICAL SIMULATIONS AND RESULTS

3.1 Numerical simulations in advance of the field test

A predictive simulation run was carried out to elaborate estimates on the potential well flow rates of gaseous CO₂ and formation water during the scheduled field-test (Martens et al., 2015). The simulation results have been considered in the planning and design of the field test, i.e., for refinement of monitoring layout and cost estimations on required brine intermediate storage and disposal. Thereafter, the valve-determined flow rates applied during the field test were used as limiting boundary condition in a second simulation run, considering the effective time schedule of the test and the maximum allowed flow rates adjusted at the release valve.

Both simulation runs were based on the history-matched reservoir model (Kempka and Kühn, 2013; Kempka et al., 2013). This calibrated reservoir model is applicable to establish reliable short- to mid-term predictions of reservoir pressure development by numerical simulations (Class et al., 2015). The Schlumberger ECLIPSE 100 black-oil simulator (Schlumberger, 2009) was employed, using a minimum downhole pressure of 59 bar at 620 m depth and atmospheric pressure conditions at the wellhead as boundary conditions for the well model in both simulation runs. An effective maximum well flow rate limit was set in the second simulation run, determined by the valve settings made during the field test to consider all manual flow rate reductions, while the first run used the scheduled maximum allowed flow rates. Since the initially scheduled and effective flow rates used in the field experiment differ in their magnitudes and time, only the results of the second simulation run are discussed in the following paragraph.

Figure 9 shows the comparison between the simulated and observed cumulative produced CO₂ and formation water. Simulated CO₂ back-production amounts to about 205 metric tonnes at the end of the field test, while the observed CO₂ back-production is about 240 metric tonnes (underestimation by about 14 %). Total co-production of brine is overestimated by about 39 % in the numerical simulations (about 91 sm³) compared with the observed coproduction (about 55 sm³). These deviations are expected to result from the wellbore model implementation, i.e., the lack of vertical flow profiles for the Ktzi 201 well, the relatively coarse lateral grid size (5 m x 5 m) in the well block elements and potential differences in the near-well (<5 m radius) CO₂ saturation. Detailed investigations are scheduled to assess the simulated gaseous CO₂ saturation in the near-well area by comparing simulation results with data from ERT and pulsed-neutron gamma (PNG) logging campaigns.

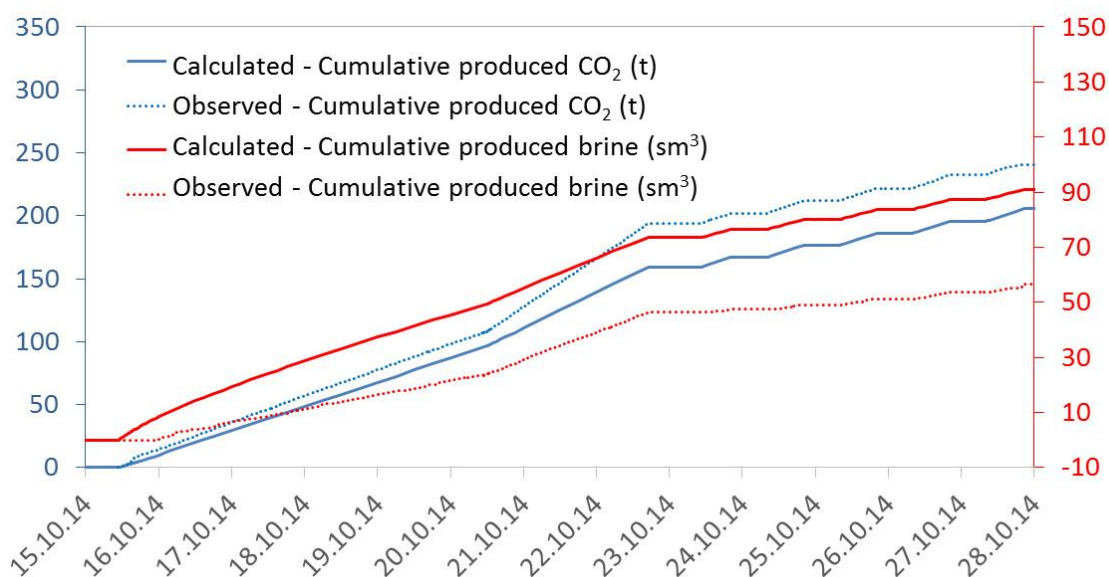


Figure 9: Comparison between the observed (dotted lines) and simulated (solid lines) back-produced gaseous CO₂ (blue lines, values on primary y-axis) and co-produced formation brine (red lines, values on secondary y-axis). Total CO₂ back-production is underestimated by about 14 %, while co-production of brine is overestimated by about 39 % in the numerical simulations based on the history-matched reservoir model of the Ketzin pilot site.

3.2 Numerical simulations after the field test (Imperial)

Imperial and GFZ made collaborative efforts to implement the Ketzin reservoir model and history match the bottomhole pressures recorded during the back-production experiment for 14 days. Scenarios of the back-production of larger volumes of CO₂ were also simulated for an extended period so as to assess the effects of associated pressure changes on the geomechanical integrity of the wellbore infrastructure and surrounding rock formation.

CO₂ back-production modelling for the Ketzin field

The back-production simulations were set up in Schlumberger’s ECLIPSE 300 (E300) software using the geological model and dynamic reservoir parameters based on previous studies carried out by Kempka and Kühn (2013). The history-matched results obtained for gas saturation and bottomhole pressures during the CO₂CARE project (Govindan et al., 2014) for the CO₂ injection period at Ketzin (June 2008 - August 2013), as illustrated in Figure 10 and Figure 11 respectively, were used in order to assume the initial reservoir condition prior to back-production.

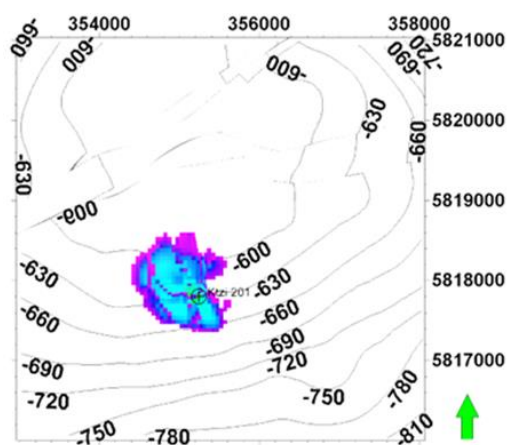


Figure 10: Simulated gas saturation distribution at the end of injection (August 2013) at Ketzi; the contour lines indicate the depth of the top surface of the reservoir model.

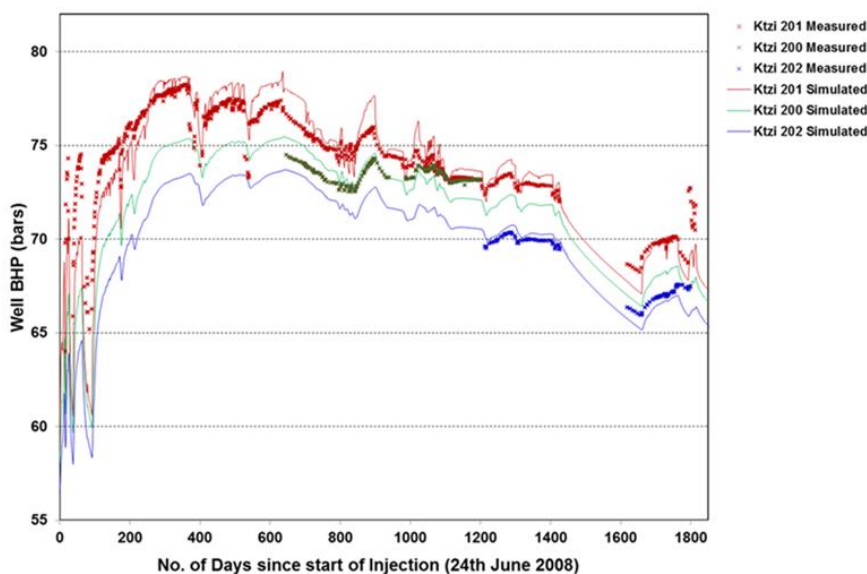


Figure 11: Comparison of measured (dotted lines) and simulated (solid lines) well BHPs during CO₂ injection at Ketzi.

The CO₂ back-production rates (in kg/hour) were implemented and the model was simulated for 14 days. It was noted that the bottom-hole temperature data did not show much variation during this period, with average values of 29.5°C and 33°C at Ktzi 201 and Ktzi 203 respectively. The history matching results for the bottom-hole pressures at the wells and CO₂ production rates obtained are illustrated in Figure 12.

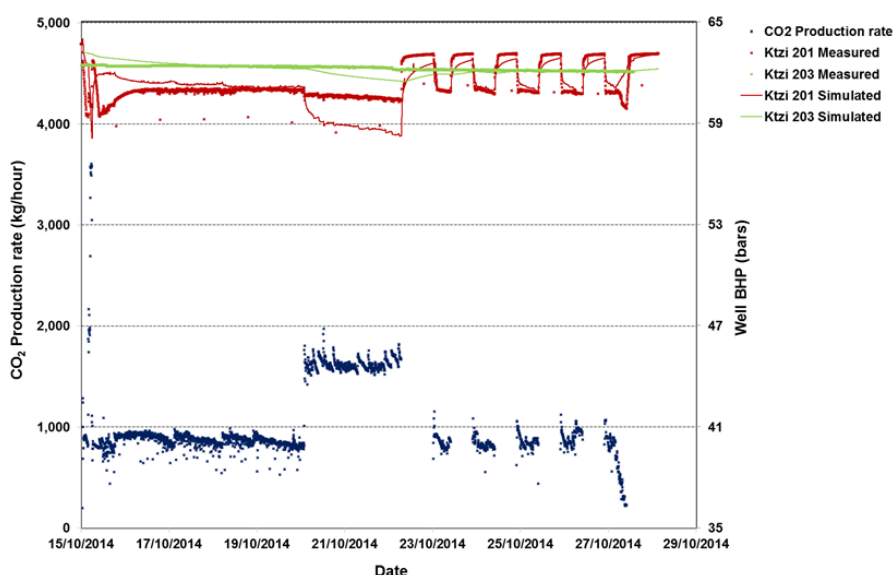


Figure 12: Comparison of the measured (dotted lines) and simulated (solid lines) well BHPs during CO₂ back-production at Ketzin.

Two scenarios were subsequently considered for extended periods of CO₂ back-production (for four months, until March 2015) including: (a) constant production rate, assumed at a peak rate of 3,500 kg/hour (**Error! Reference source not found.**); and (b) ariable production rate, switching periodically between 0 and 3,500 kg/hour every month (Figure 14). The results for the simulated bottom-hole pressures at Ktzi 201 indicate that the change in pressure would range between 10-40 bars in these long-term back-production scenarios.

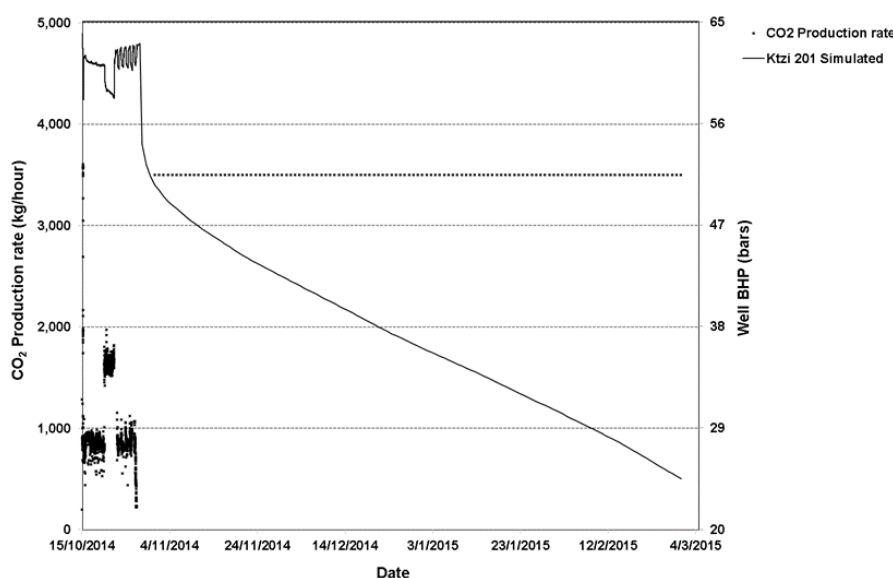


Figure 13: Simulated long-term well BHP at Ktzi 201 for a scenario considering CO₂ back-production at a constant rate.

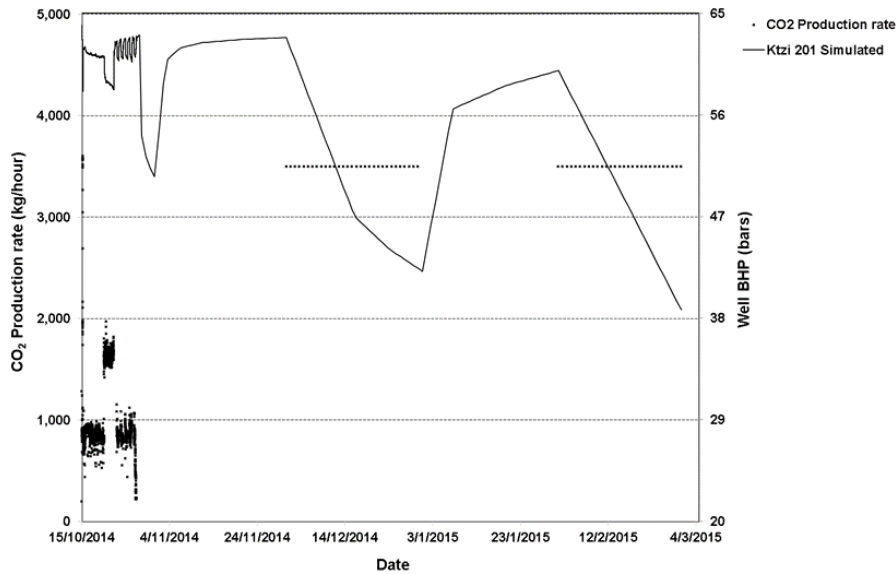


Figure 14: Simulated long-term well BHP at Ktzi 201 for a scenario considering CO₂ back-production at a variable rate.

Near wellbore geomechanical model for the Ketzin field

The near wellbore model developed aims at assessing the potential for failure zone development during both CO₂ injection and back-production period at the Ketzin site. Since the temperature monitoring results suggested that there was no significant temperature change during the operational period, only the effect of pressure change on near wellbore behaviour was considered in this model.

As illustrated in Figure 15, increasing pore pressure may push the Mohr circle beyond the failure envelope and result in shear failure. Excessive pressure increase ($p > \sigma_3$) can also induce tensile failure and thus fracture the reservoir. On the other hand, reducing the pore pressure moves the Mohr stress circle further away from the Mohr failure envelope, which makes failure less likely to happen.

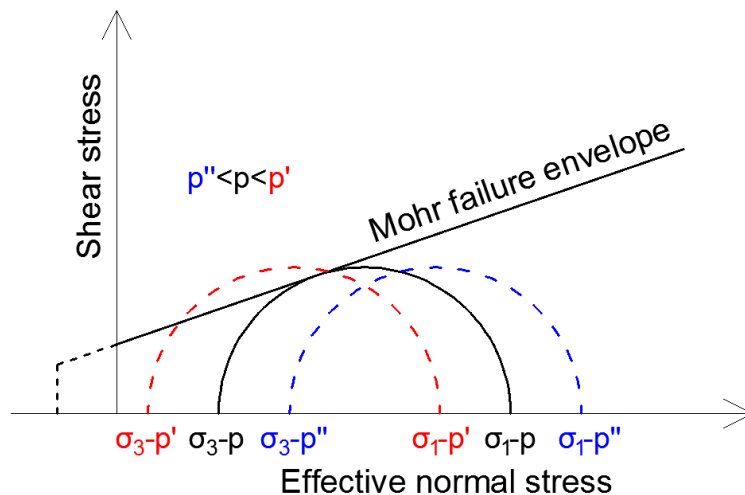


Figure 15: Pore pressure dependent failure behaviour of rock formations.

Model development

Numerical models to assess near wellbore stress and failure behaviour during CO₂ injection and back-production at Ketzin were developed in FLAC^{3D}, an advanced geomechanical analysis software. As shown in Figure 16a, the physical dimensions of the model are 10×10×10m (length×width×height) and a cylindrical zone at the centre of the model is refined to accommodate the simulated wellbore. Figure 16b shows the detailed model design of the near wellbore, which covers two concentric rings of cement and casing. The entire model domain was assumed to be within the Stuttgart formation at depth from -640 to -650 m.

In the model, the σ_v is assumed to be the intermediate principal stress and its magnitude is close to the load induced by overburden weight, which is 15.1 MPa. As reported by Klapperer et al. (2011), the maximum principal stress σ_H is in NE-SW direction parallel to the axis of the anticline. The magnitudes of σ_H and σ_h are suggested to be lower than $2.8 \sigma_v$ and higher than $0.62 \sigma_v$, respectively. Therefore, σ_H and σ_h are assumed to be the maximum (42.3 MPa) and minimum (9.4 MPa) values at each range. Y-axis was assumed to be the vertical direction, z-axis (positive) was assumed to be pointing the North, and the angle between σ_H and z-axis is 60°. The boundary conditions of the model were such that it is laterally confined and the model base is fixed.

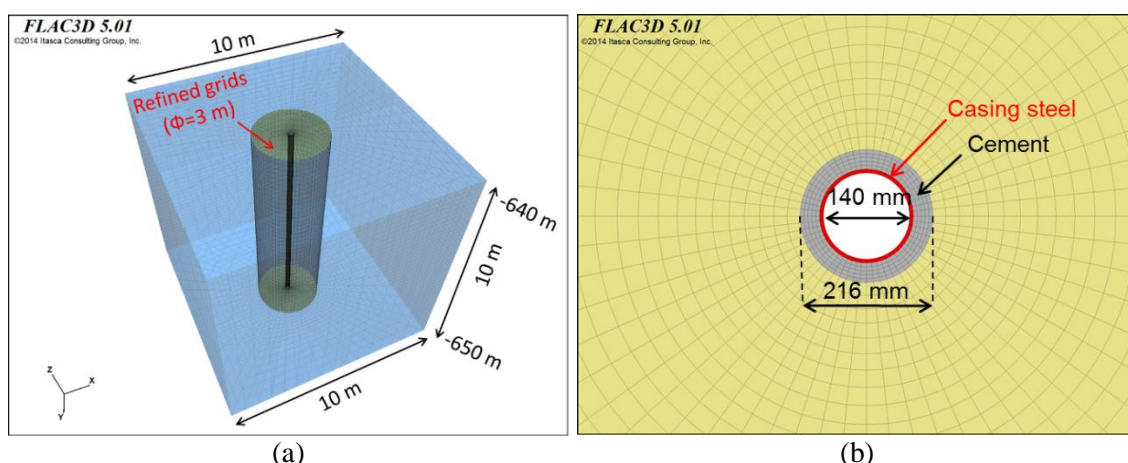


Figure 16: Model geometry and the central refined area.

Table 2: Rock mechanical and strength properties of the Stuttgart formation and the wellbore material.

Layer	K (GPa)	G (GPa)	φ (°)	C (MPa)	t (MPa)
Stuttgart formation	6.06	3.13	25	11.47	-1.15
Cement	19.43	6.14	-	-	-
Casing steel	160.31	80.47	-	-	-

Rock mechanical properties used in this model, which are summarised in Table 2, were adopted from the paper published by Ouellet et al. (2011). The constitutive model used here was assumed to be the classical Mohr-Coulomb model in FLAC^{3D}. Cement and casing steel were modelled as elastic and their properties are based on literature (BGS, 2008). The initial reservoir pore pressure was assumed to be uniform at 6 MPa within the model domain.

The simulation consists of five consecutive procedures: (1) initial equilibrium, (2) well drilling, (3) wellbore completion, (4) CO₂ injection, and (5) CO₂ back-production. Well drilling was simulated in the model by assigning the ‘NULL’ property (no mechanical stiffness and strength) to the grids representing the well at 216 mm diameter. In the wellbore completion stage, the grids representing the cement and casing were reinstated and the well diameter was reduced to 140 mm. The coupling between casing and cement, cement and rock were simply assumed to be fully bonded.

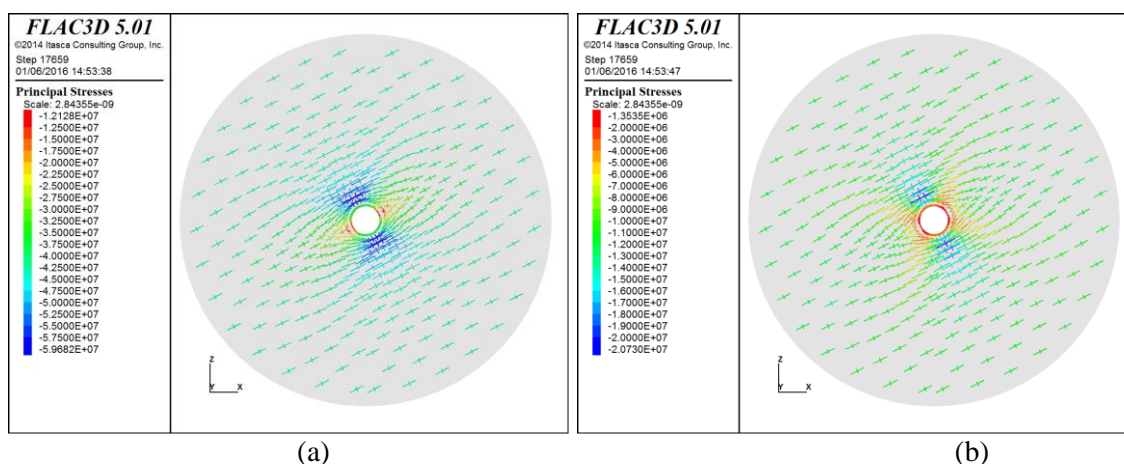


Figure 17: Principal stress tensors after well completion: (a) tensors coloured by the maximum principal stress and (b) tensors coloured by the minimum principal stress.

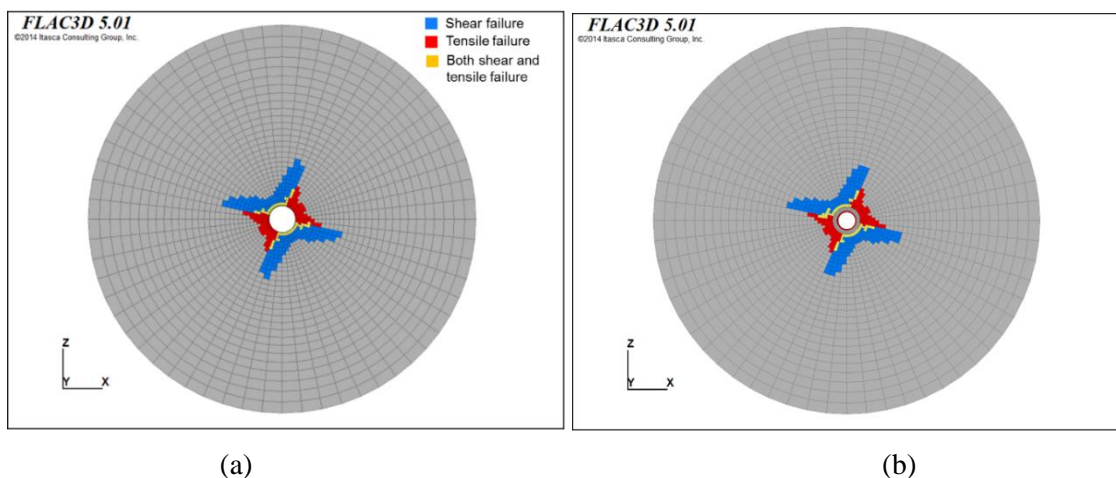


Figure 18: Near wellbore failure zones after (a) well drilling and (b) well completion.

The stress distribution estimated after well completion is shown in Figure 17. As expected, in the near wellbore grids, notable stress concentration can be observed along the direction of minimum principal stress. On the other hand, along the direction of maximum principal stress, near wellbore grids experienced dramatic stress relief. As a response to the stress change, the failure zone near the wellbore is presented in Figure 18, which forms the baseline for further injection/backproduction processes. Shear failure was shown in the large compressive stress zone and tensile failure was found in the stress relief zone. Well completion process has no direct impact on the development of near wellbore failure zone.

Geomechanical response to CO₂ injection and back-production

Near wellbore stress and failure behaviour during the CO₂ injection phase was first evaluated. The pore pressure within the model domain was gradually elevated from 6 MPa to 8 MPa to simulate the CO₂ injection process. In the meantime, the percentage of failure zone volume within the refined area was recorded at different pressure levels (see Figure 19). As shown in Figure 19 and Figure 21, the failure zone size near the wellbore increased slightly with the increase of CO₂ injection pressure.

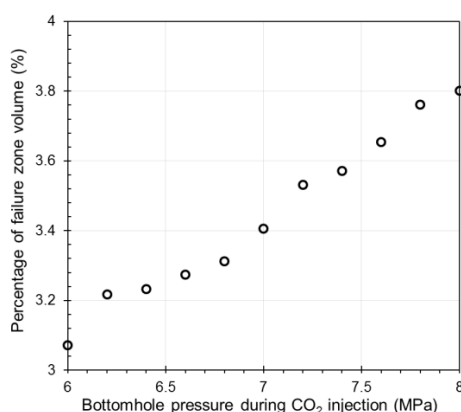


Figure 19: Failure zone development during the CO₂ injection process.

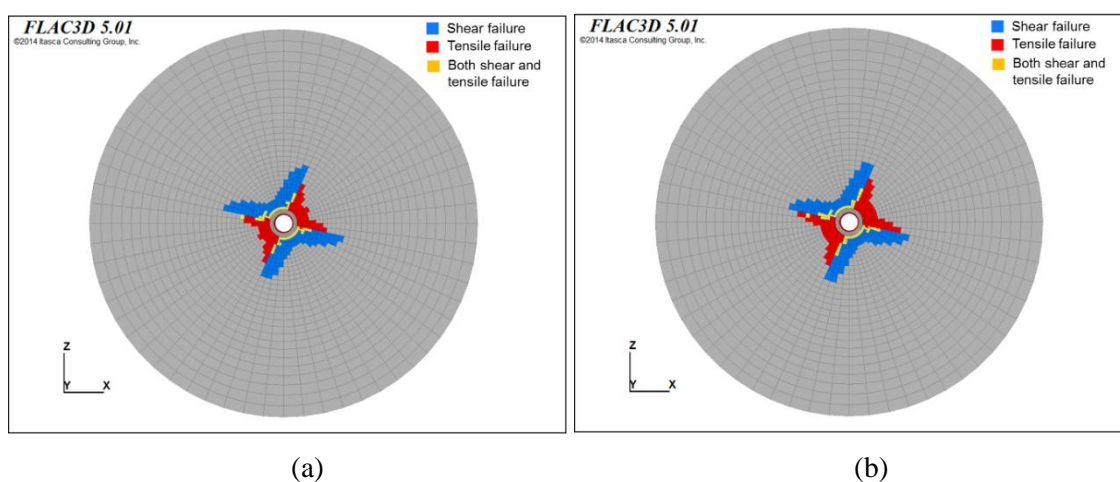


Figure 20: Distribution of the near wellbore failure zone when the CO₂ injection pressure is (a) 7 MPa and (b) 8 MPa.

Next, the wellbore model was used to reduce the pore pressure gradually from 8 MPa to 4 MPa to mimic the period of CO₂ back-production.

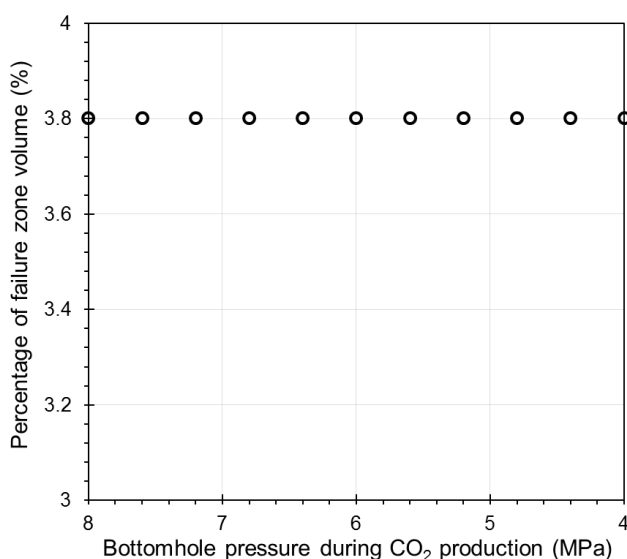


Figure 21 illustrates that decreasing the near wellbore pore pressure has almost no effect on the failure zone developed earlier, and its size remains the same after CO₂ back-production.

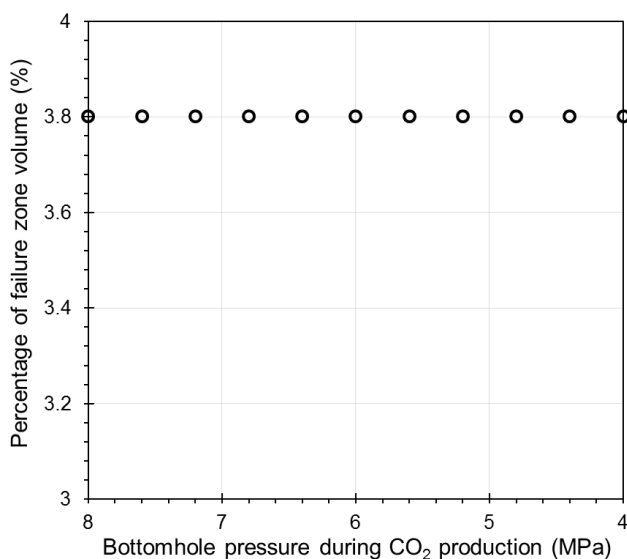


Figure 21: Failure zone development (or lack of it) during the CO₂ production process.

3.3 Development of an inverse Ketzin model for near-wellbore studies (GFZ)

Previous Ketzin reservoir modelling work focused on reservoir CO₂ pressure and arrival times (Kempka and Kühn, 2013). It captured the arrival times and the long term trend of CO₂ reservoir pressure reasonably well. This model significantly underestimates short term variations wherefore the modelling was strongly constrained with observation data. Therefore, it was decided that the CO₂ back-production experiment should be modelled

during the MiReCOL project. The modelling work includes short term pressure variations with time scales from hours to days. The predictive capabilities of this kind of models partly rely on data that is observed after the experiment. Consequently a model with improved short term behaviour was developed.

Back-production of CO₂ is connected with shifting the brine/CO₂ interface. Brine is accumulated by coning in the vicinity of the wellbore. This effect is theoretically known and described for natural gas production. However, this experience cannot be directly applied to CO₂ back-production (Liebscher et al., 2016) and should be investigated in detail with the in situ condition of reservoir. Therefore, the new model aims to include resistivity data for an improved imaging of near wellbore changes in saturation.

A novel inverse model has been established for the Ketzin pilot site. It integrates three pre-CO₂-injection hydraulic tests and the first 270 days of CO₂ injection. It comprises 500 free parameters and is feasible to model channeling effects due to layered permeability. It is an advanced continuation of the hydraulic modelling work of Chen et al. (2014) and forms a necessary complement for description of near wellbore effects and consistency with hydraulic testing, which is not covered by the recent large scale Ketzin model. The task requires high technical prerequisites: Coupling of a single phase model with a multiphase model, coherent time stepping adaptation during the inversions, online observation of model results during runtime. A significant reduction of model runs could be achieved by application of singular value decomposition assistant. In the last report period the model was extended to a full hydrogeophysical inversion environment.

The hydrogeophysical inversion framework is shown in **Error! Reference source not found.** The parameter estimation Tool PEST forms the central part. An initial permeability field is generated based on user setting. Based on an empirical petrophysical relation (Norden and Frykman, 2013) this is transferred to a porosity field. These two fields form the main input data to hydraulic simulation with Eclipse 100 and multiphase CO₂ simulation with Eclipse 300. These models generate hydraulic data and CO₂ pressure, which are compared to their respective observation counterpart. Eclipse 300 furthermore generates a spatial CO₂ saturation which forms the input to the geoelectrical simulations carried out with pyGIMLi.

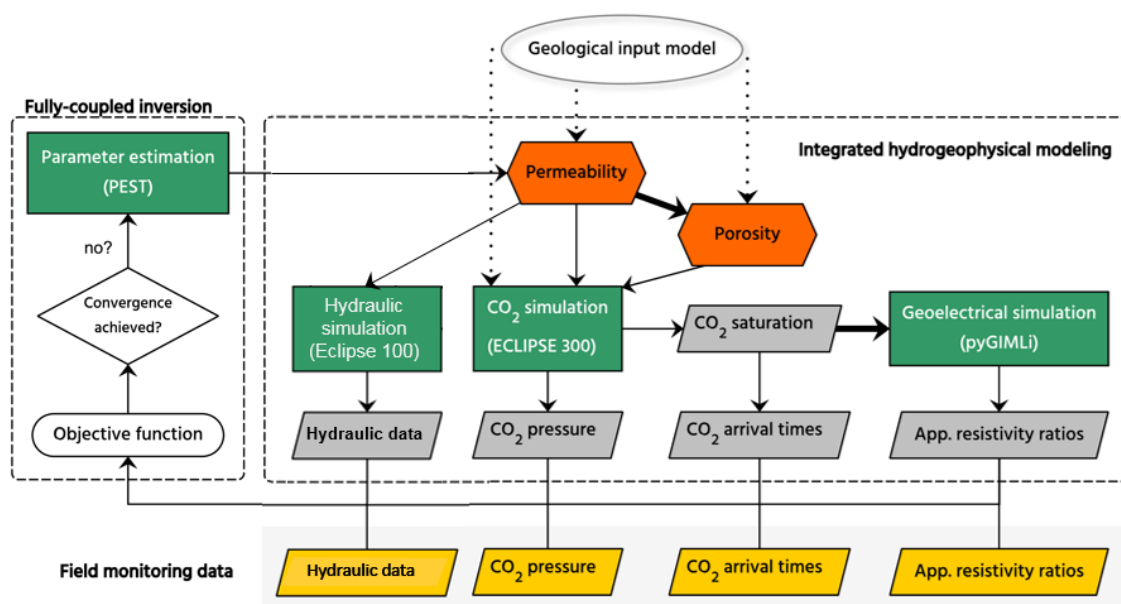


Figure 22: Flow chart of the hydrogeophysical inversion framework. Green fields indicate active modelling tools, orange field indicate parameter fields, grey fields show simulated physical properties. Monitoring data are represented by yellow fields.

The model is spatially parameterised with a pilot point approach. Pilot points are spatially distributed over the model area with each pilot point representing one model parameter. They form a grid on top of the numerical model grid. Hydrological parameters i.e. permeability or porosity are interpolated between the pilot points and assigned to each model cell. This resulting parameter fields are closer to reality than using traditional zonation approach which was applied by Chen et al. (2014).

The pilot points are heterogeneously distributed with higher density in areas with much information, i.e. in vicinity to the wells and lower density in at larger distances (**Error! eference source not found.**). The same principle applies to different lithological units. The higher importance of the aquifers relative to the aquitards is honoured by higher pilot point density (**Error! Reference source not found.**).

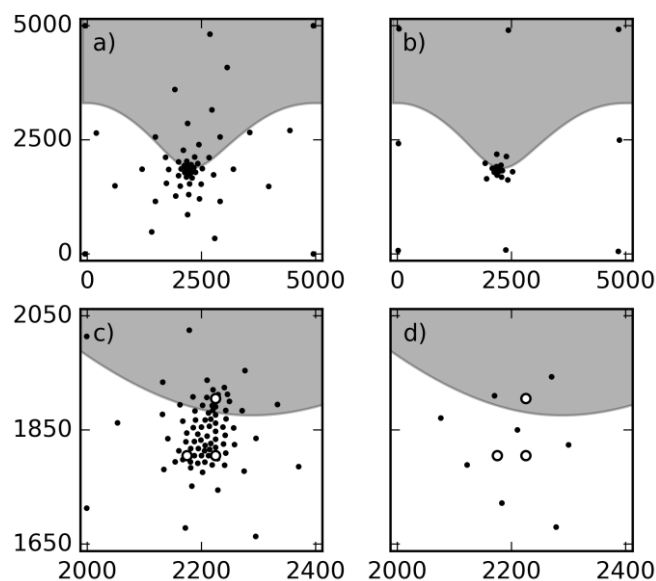


Figure 23: Permeability parameterisation of model layers with spatially distributed permeability. Dots indicate pilot points, circles indicate the wells, which are pilot points as well. The main reservoir aquifers (a,c) are discretised by 194 pilot points, the aquitard anhydrite layer (b,d) is discretised by 25 pilot points. The grey area indicates a low permeability area. The scale is in metres from the model origin, subplots c and d are details from subplots a and b, respectively.

Convergence problems of the hydraulic model have been addressed. Previous versions of the model resulted in very heterogeneous parameter distributions. A detailed analysis shows that two (obs200_p201, obs201_p200) of nine hydraulic time series are mutually exclusive, only either of them can be calibrated. This is surprising since both are reciprocal, i.e. only pumping and observation well are switched. Furthermore, when including one of the abovementioned time series the calibrated permeability is outside the range of realistic values that can be expected in the reservoir (Figure 24). Time series obs200_p201 and obs201_p200 were recorded consecutively with the same data logger, which was just shifted from one well to the other. Consequently, both time series are removed from the dataset.

The reduced set of observations results in better inversion convergence. Simulations based on the entire dataset show pronounced artifacts in the permeability distribution (Figure 25 **Error! Reference source not found.**a). The parameters hit their upper and lower boundaries, the high permeability contrasts appear unrealistic. In the model, the near wellbore permeabilities are constrained to their observed values which are comparatively similar (Norden et al., 2010).

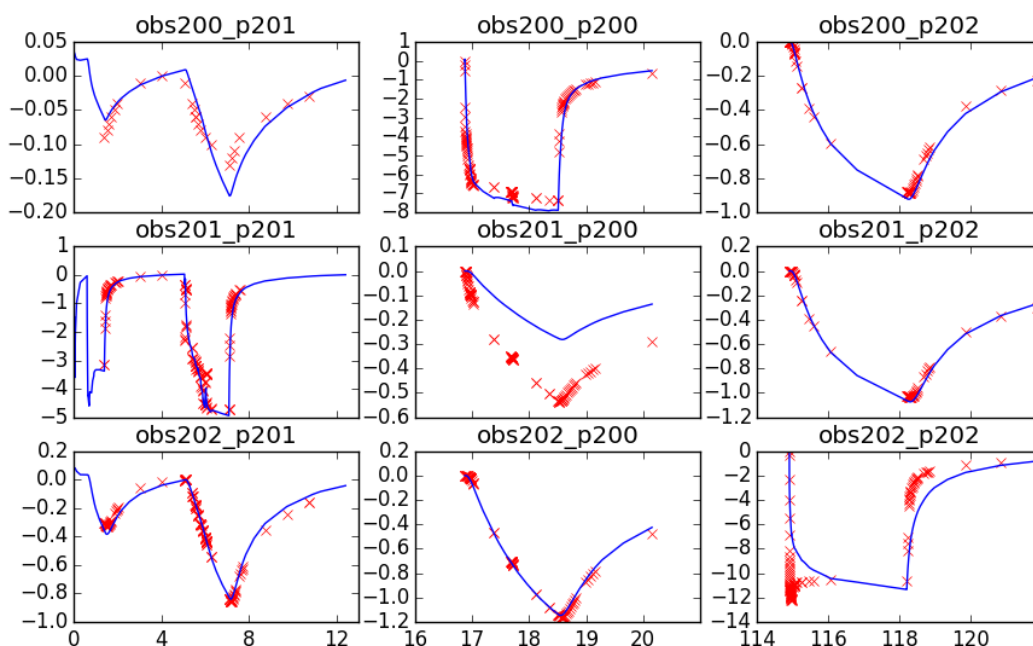


Figure 24: Results of the hydraulic model. The x axis shows days since the first pumping test, the y axis shows drawdown. Red crosses indicate observed, blue lines indicate simulated values. The first part of the subplot titles indicate the observation well, the second part the pumping well, e.g. obs200_p201 are hydraulic observations in well Ktzi200 during pumping in well Ktzi 201.

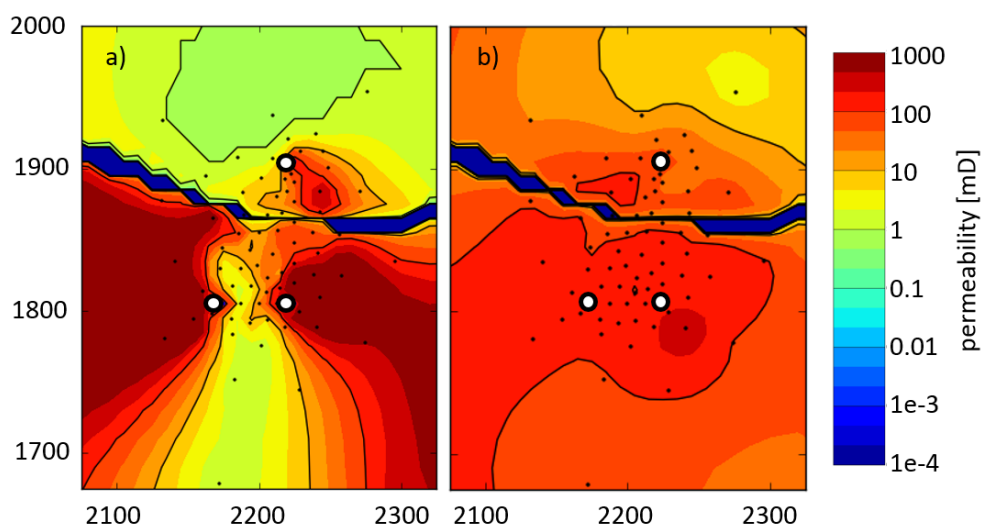


Figure 25: Calibrated permeability distribution a) including all hydraulic time series b) excluding time series obs200_p201 and obs201_p200. The white circles indicate wells, the black dots indicate pilot points. Map units are metres from the model origin.

In the resulting parameter map the wells are located at the inflection points of the permeability (Figure 25a). It appears arbitrary that the wells penetrate just the areas with average permeability. The permeability distribution in **Error! Reference source not found.** Figure 25b is more realistic. The contrasts within the aquifer are similar to the permeability contrasts observed in the wells. Although it might be critical to exclude incompatible observations from a model, these indications appear strong enough that the respective observations are considered as erroneous.

Significant progress was made in including electrical resistivity tomography (ERT) into the model. The pyGIMLi geoelectrical forward code was coupled successfully into the inversion framework (**Error! Reference source not found.**). While convergence for the individual data types hydraulics, CO₂ pressure and arrival times can be achieved, the convergence of geoelectric data is not satisfying. The observations show a higher dynamic than simulated values. Exemplarily one of over 1000 electrode configurations is shown in (**Error! Reference source not found.**). The next step is to find an appropriate data filtering criterion. Although the reciprocal observations should match and provide identical values, there is typically a certain mismatch between the data. For the current example in **Error! Reference source not found.** both curves show the same dynamic, but the signal of the reciprocal configuration (blue curve) is about twice as high compared to the base configuration (green curve). The example of hydraulic data described above emphasizes that unreliable data can cause significant deterioration of the model performance. Consequently, further investigation will identify appropriate statistical criteria for selecting only the most reliable data for the inversion.

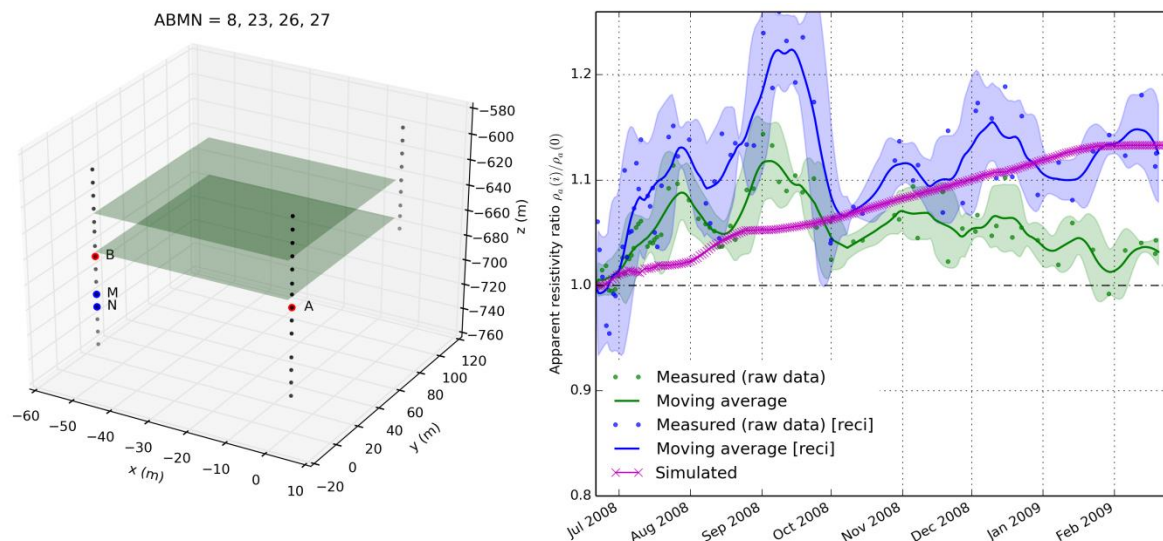


Figure 26: The left part shows the current electrode configuration. Red circles indicate current injection electrodes, blue circles indicate voltage observation electrodes. Grey dots indicate inactive electrodes attached to the borehole casing. The right part shows the apparent resistivity ratio. Observed values have green and blue colour, simulated values are presented in pink.

4 PRACTICAL UNDERSTANDING OF WELL LOAD-UP BEHAVIOUR

4.1 Well effects during back-production

Assessing the feasibility of CO₂ back-production from a storage reservoir does not only require knowledge of the near-well and far-field reservoir behaviour but also of the in-well conditions.

As shown in report D4.1, the back-production of CO₂ reverses the flow direction and multiphase flow phenomena occur that are fundamentally different as those from the injection. The back-production phase can be described by three different operational modes, depending from the actual production rate r_{CO_2} (Table 1, Figure 27). At reservoir elevation both, CO₂ and brine are extracted from the sandstone. The water has a higher density than CO₂ and remains in the lower part of the well where it re-infiltrates into the formation. Therefore a water cone develops as seen in **Error! Reference source not found.**

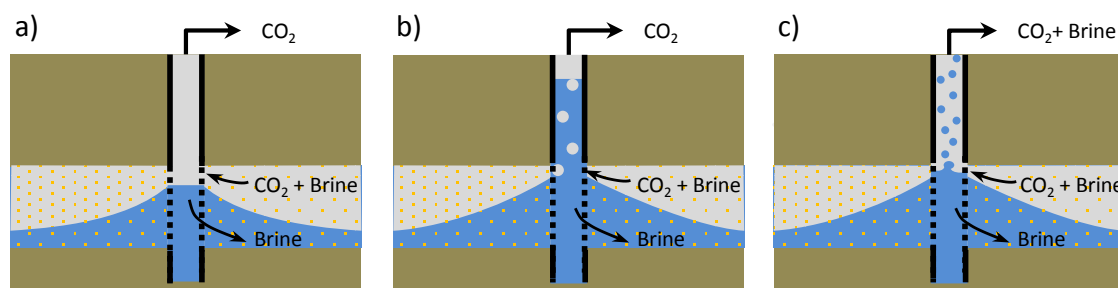


Figure 27: Three operational modes during the back-production test: (a) At low production rates $r_{CO_2} < r_{c1}$, pure CO₂ can be produced continuously at wellhead elevation. (b) At production rates $r_{CO_2} > r_{c1}$, the water level rises above the well filter and the CO₂ passes through the water column in form of bubbles. (c) In case the production rate exceeds the Turner velocity ($r_{CO_2} > v_{Tur}$), the brine is dispersed and entrained by the CO₂, transported upwards and arrives at the wellhead.

4.2 Turner criterion

The back-production experiment was monitored by continuous pressure and temperature measurements in the producing well at 550 m depth at the lower end of the production tubing – i.e. ~ 80 m above the reservoir – and at the wellhead; flow rate of the produced stream was measured by a Coriolis type mass flow meter and controlled by a choke manifold. After initial commissioning and testing of the equipment during the first hours, the experiment was performed in three main stages: Continuous operation with mean flow rates of ~ 800 kg/h from 15th to 20th October 2014 and ~ 1,600 kg/h from 20th to 22nd October and an alternating regime from 22nd to 27th October with a mean flow rate of ~ 800 kg/h during day shift and shut-in during night shift. At the end of the experiment flow rate was ramped down over 6 hours in 100 kg/h steps from 800 kg/h to 200 kg/h. Throughout the back-production downhole pressure and temperature conditions were very stable at ~ 29 °C/61 bar as was wellhead pressure at ~ 46 bar; wellhead temperature showed stronger variations reflecting day-night

changes of ambient air temperature and solar radiation. The actual measured downhole and wellhead pressure and temperature data for density calculations were used based on an EOS for pure CO₂ in combination with inner wellbore diameters of 73 mm for the production tubing and 121 mm for the production string to calculate minimum (critical) gas flow rates and velocities according to the Turner criterion as developed for natural gas-well load-up.

For the 5^{1/2}" casing, the calculated minimum (critical) velocities based on the Turner criterion are notably higher (up to one order of magnitude) than the actual velocities during the back-production experiment, wherefore well load-up was expected (Figure 28). However, the very stable downhole pressure conditions precludes any well load-up due to accumulation of reservoir brine below the production tubing indicating that flow rates were high enough for entraining any co-produced reservoir fluid to the surface. This is supported by a constant gas/fluid ratio during the different rate stages of the experiment. The data suggest that it is not sufficient to change EOS based fluid properties of a traditionally developed Turner criterion that is adjusted to natural gas production. The criterion still overestimates the minimum (critical) velocity for fluid entrainment in a CO₂ dominated well. For future experimental and operational design it is required to modify the entire set of empirical parameters to calculate an accurate Turner criterion.

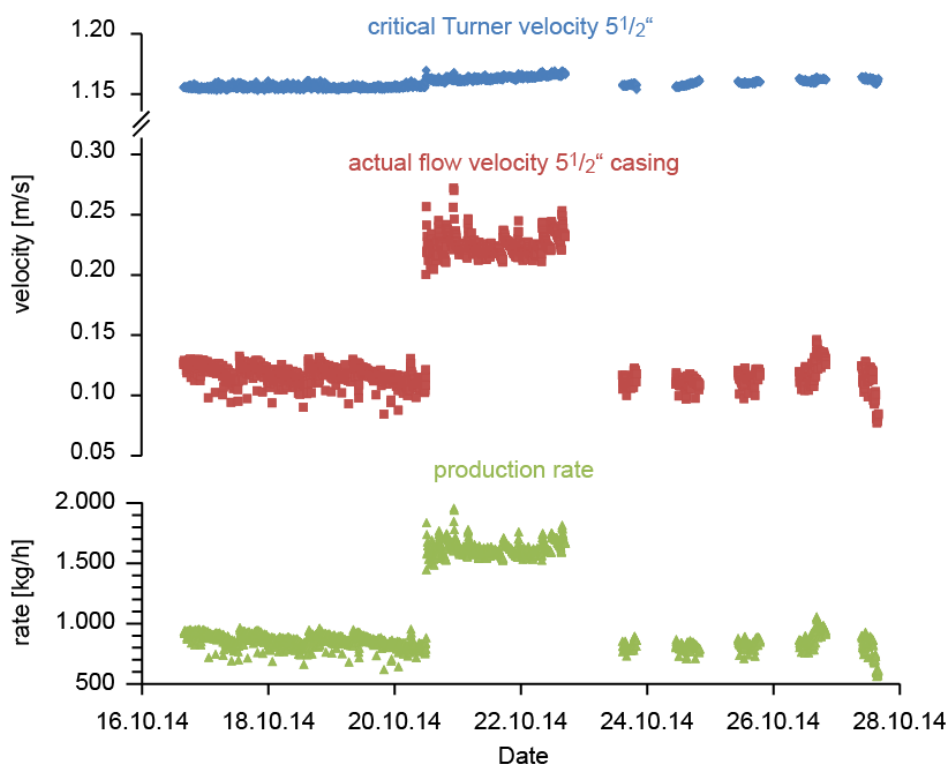


Figure 28: Calculated critical Turner velocity (blue) compared to actual flow velocity (red) for the 5 1/2" casing. The actual flow velocity positively correlates with production rate (green) but is notably lower than calculated critical Turner velocity throughout the entire back-production experiment.

5 CASE STUDY OF THE K12-B GAS FIELD

5.1 Field site

The K12-B gas field is located in the Dutch sector of the North Sea, some 150 km northwest of Amsterdam (Figure 29). It has been producing natural gas from 1987 onwards and is operated by Engie E&P Nederland B.V.

The K12-B structure was discovered in 1982 by the K12-6 exploration well. Gas production started in 1987. Gas is produced from the Upper Slochteren Formation of Permian age (Rotliegend). The reservoir lies at a depth of approximately 3800 meters below sea level, and the temperature of the reservoir is about 128 °C. The gas contains 13% CO₂ which is removed from the gas stream at the production platform. Gas is produced from the Upper Slochteren Formation of Permian age (Rotliegend). The K12-B gas reservoir is the first and so-far only gas reservoir in the Netherlands in which industrially produced and captured CO₂ was re-injected in the reservoir. The K12-B field consists of several compartments that are hydraulically separated by several faults. The current investigation concentrates on compartment 4, where two back-production operations have been carried out. More info on the CO₂ injection at this site can be found in Vandeweijer et al, 2011 and Van der Meer et al, 2009.

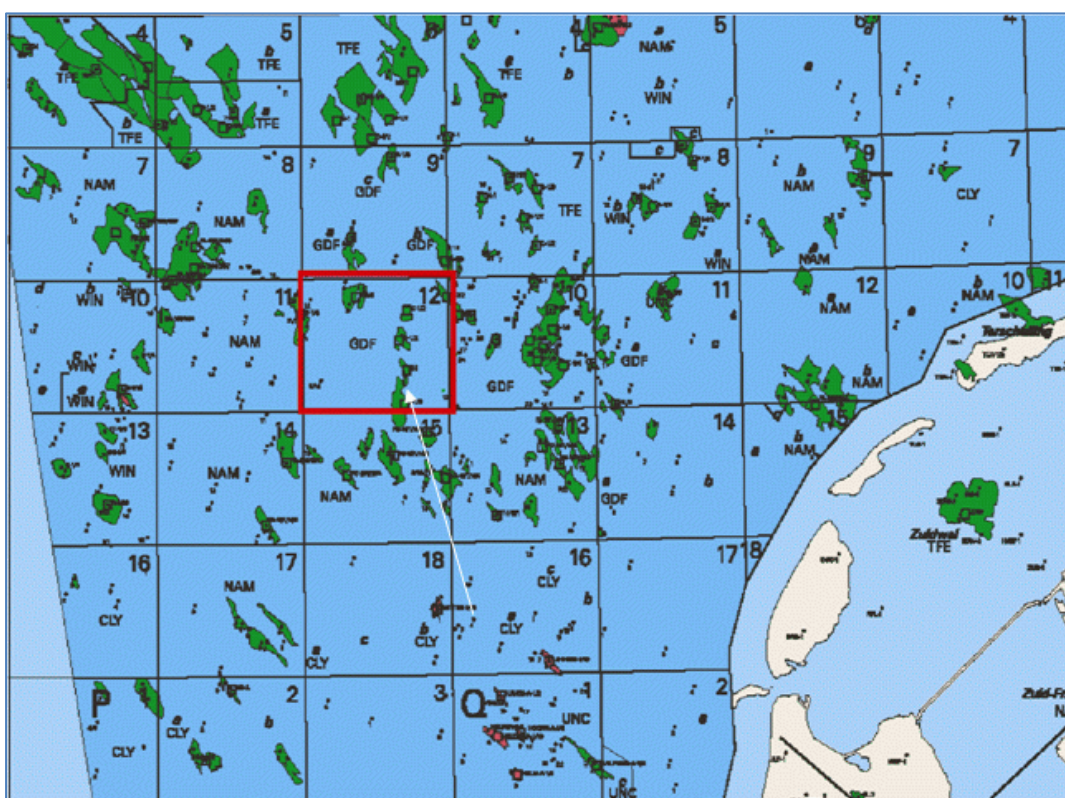


Figure 29: Location of the K12-B reservoir in the Dutch part of the North Sea (supplied by operator).

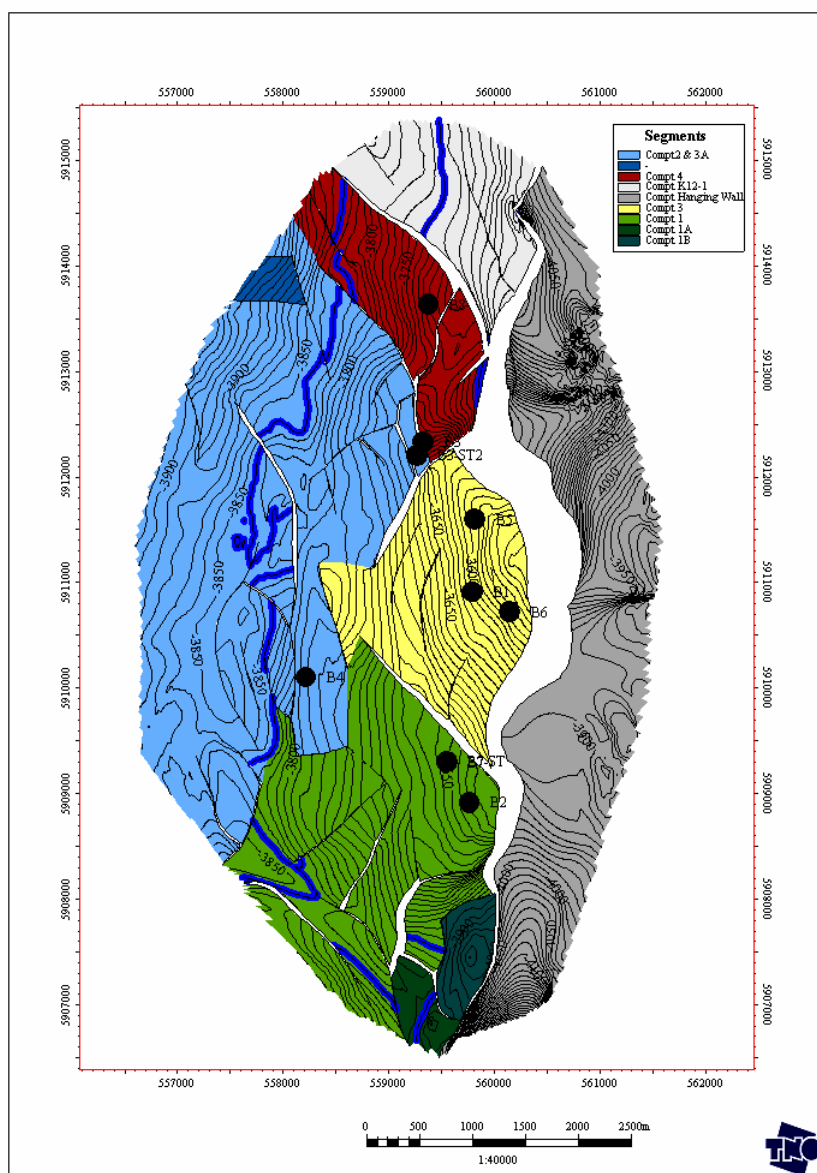


Figure 30: Compartment structure of the K12-B gas field. Compartment 4 (dark red) is under investigation in this report. Wells are indicated by black circles, with B8 located in compartment 4 (modified after Vandeweijer et al., 2008).

5.2 Back-production experiments

In 2004, the well K12-B8 had ceased conventional gas production and was converted into an injection well. More than 10 kt CO₂ had been injected into compartment 4, and after that, well B8 was closed again (Vandeweijer et al, 2008). The well was re-opened at the end of 2007, and significant amounts of CH₄ and CO₂ were produced simultaneously. After one year, the production stopped again. In 2012, a further CO₂ injection period was carried out, followed by a brief back-production period in 2014.

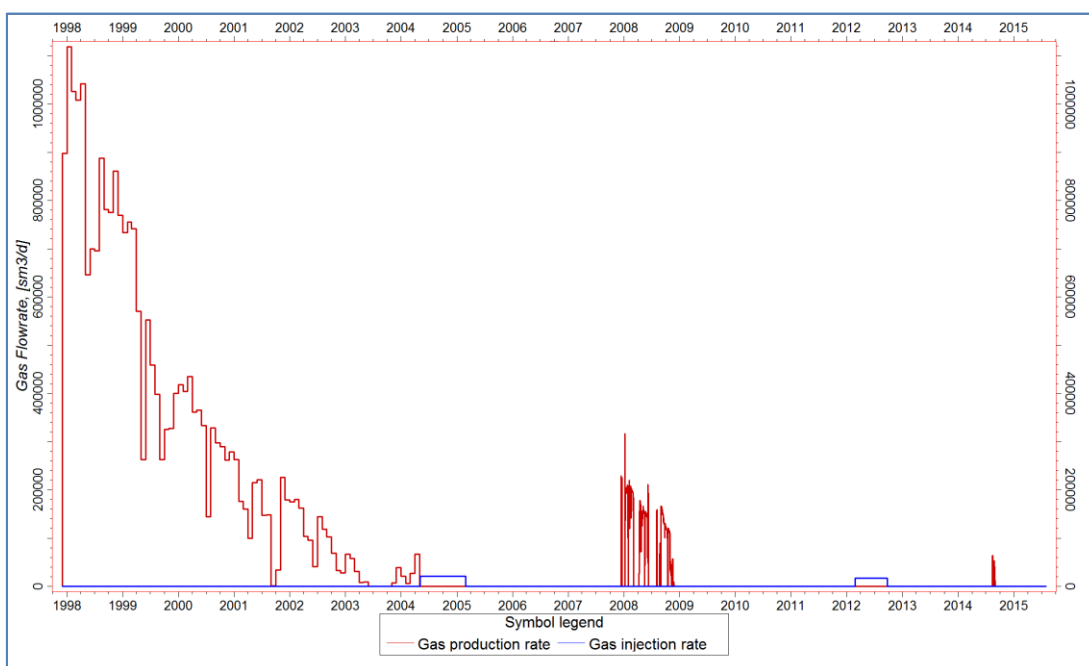


Figure 31: Gas production (red) and CO₂ injection rates (blue) in the well B8 as supplied by the operator. Back-production periods are from the end of 2007 until the end of 2008 and also in late 2014.

The water production was not measured individually for compartment 4, but values were measured at the separator for the entire field. The water rate was around 40 m³/mlnNm³ (40 m³ water in 1 million m³ gas at 0°C and 1.01325 Bar), with a low salt content. This indicates that the K12-B aquifers were in not-active state. The water was probably a result of condensation at the surface from the wet gas due to decreasing temperature and pressure.

When well B8 was put in back-production in December 2007, the well head pressure (WHP) was significantly higher than that at the time of the end of the CO₂ injection (early 2005, see Vandeweijer et al, 2008). This indicates that the compartment and its gas had been under influence of processes not formerly taken into account. Potential underlying processes are: (i) leakage from neighbouring/internal compartments, (ii) not yet identified sub-compartments, (iii) leakage from tighter parts of the reservoir, (iv) aquifer support or (v) compaction. A combination of the processes is possible.

5.3 Modelling approach

The geological model is based on the general K12-B static model (Van der Meer et al, 2005). To avoid as much water production as possible a vertical permeability anisotropy k_v/k_h of 0.1 was used and all faults were closed, with the exception of Faults 2, which had a limited transmissivity of 0.1.

The compositional reservoir simulator Eclipse 300 was used for simulations. The PVT (pressure-volume-temperature) model was taken from a previous study on compartment 3 of K12-B. Production and injection data for the compartment were received from the

operator. Figure 31 shows the various production and injection procedures, which took place in compartment 4. The schedule of the history match was based on these production and injection data. The history match was conducted using the supplied gas production and injection rates as constraints.

Data on the composition of the produced gas during the first back-production were taken, as well as further observations during that test were taken by Vandeweyer et al, 2008. From the second back-production tests, only indirect observations, such as short duration and high CO₂ concentrations, were available (supplied by operator). Other observations from K12-B (such as actual gas-water-ratios) were also obtained from the operator ENGIE.

5.4 Results

Error! Reference source not found. shows the simulated gas and water production rates. The maximum simulated water production is around 120 m³/mlnNm³ and drops with the reduced gas production rates. This is considerably higher than the observed value of 40 m³/mlnNm³. A possible explanation is the high salinity of the reservoir fluid. Although the ratio of free water is negligible, a considerable amount of pore water is present. Therefore, the vapour pressure in the gas is in equilibrium with this pore water. The high salinity of the pore water reduces the vapor pressure, and therefore, the water content in the gas compared to low salinity conditions (Panin and Brezgunov, 2006). The vapour pressure in the reservoir simulator is not a function of pore water salinity but is referenced to freshwater conditions. Therefore, the simulations overestimate the vapor pressure, and as a result the water production rate.

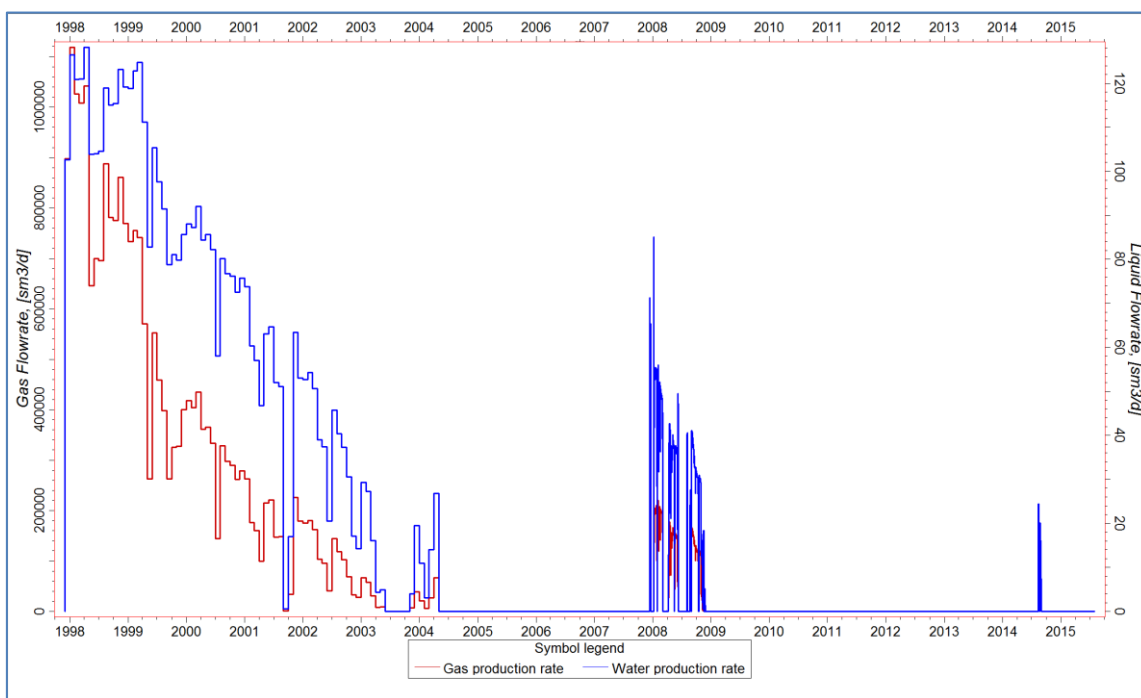


Figure 32: Simulated gas production rate (red) and water production rates (blue).

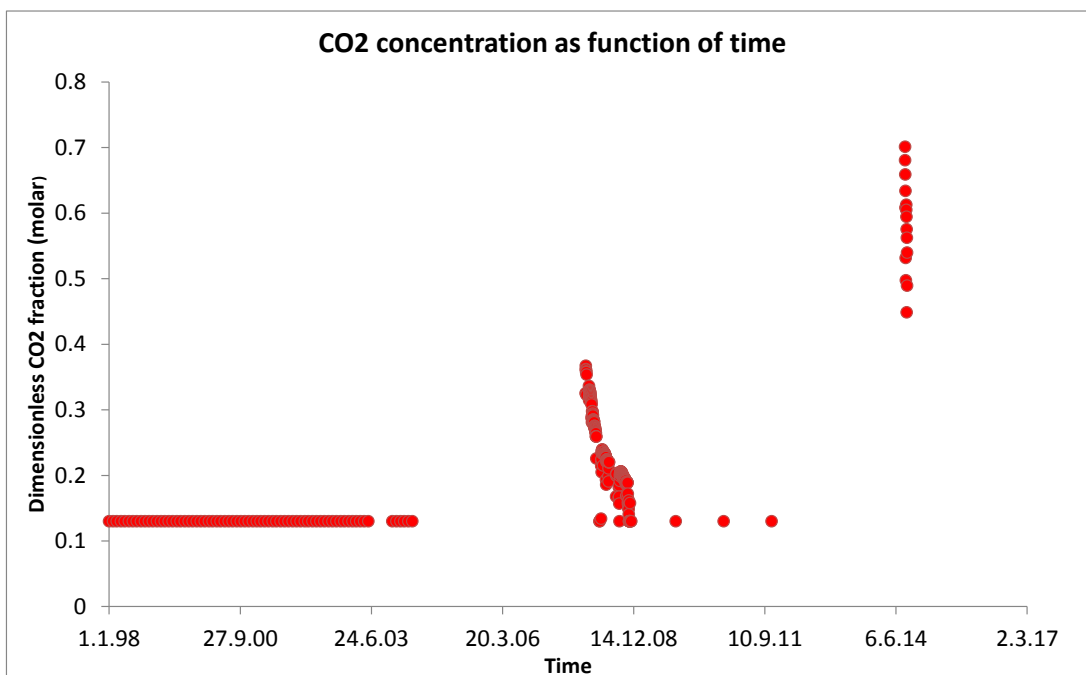


Figure 33: Simulated CO₂ mole fraction of the produced gas, as function of time.

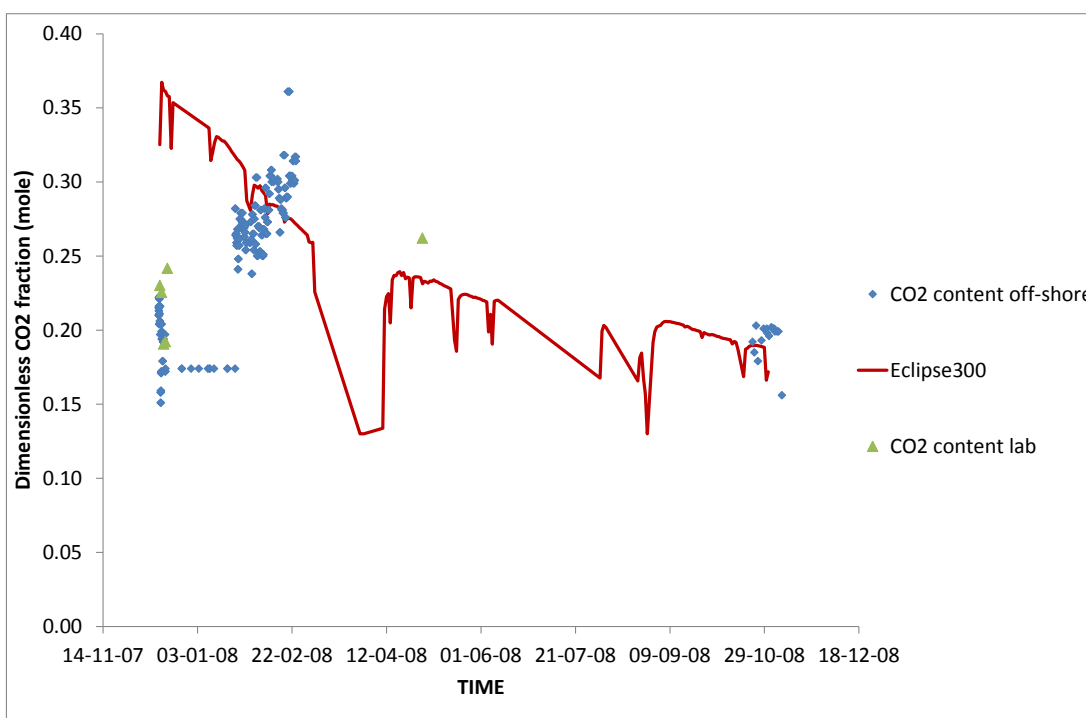


Figure 34: Simulated (red line) versus measured (green for lab analyzed gas samples, and blue for in-situ detection at the platform) CO₂ molar fractions during the first back-production experiment.

The measured CO₂ content data of the off-shore detection equipment was assumed to be based on molar fractions. Comparing the simulated CO₂ concentration with the measured values (Figure 34) indicates that the simulated CO₂ concentration in the produced gas is initially higher than the measured values. This can probably attributed to more distinct spreading and dispersion of the CO₂ in reality in comparison to the simulations.

The second group of measurement were taken around November 2008 (Figure 34), which is 11 months after the start of the resumed production. The measured value of 0.2 again are similar to the simulated values at that time.

The CO₂ content remains constant during the 2.5 years after the first back-production period (Figure 33). Careful examination of the production rates revealed production rates of very short duration during that period. Apparently the operator was attempting to reopen the well B8 during this period.

Figure 33 shows that the simulated CO₂ mole fraction in the second back-production period is 0.7. The measured concentrations for the second back-production experiment were in the range of 0.45-0.5. This indicates that the spreading away of from the well B8 is more pronounced in reality than simulated by the reservoir model.

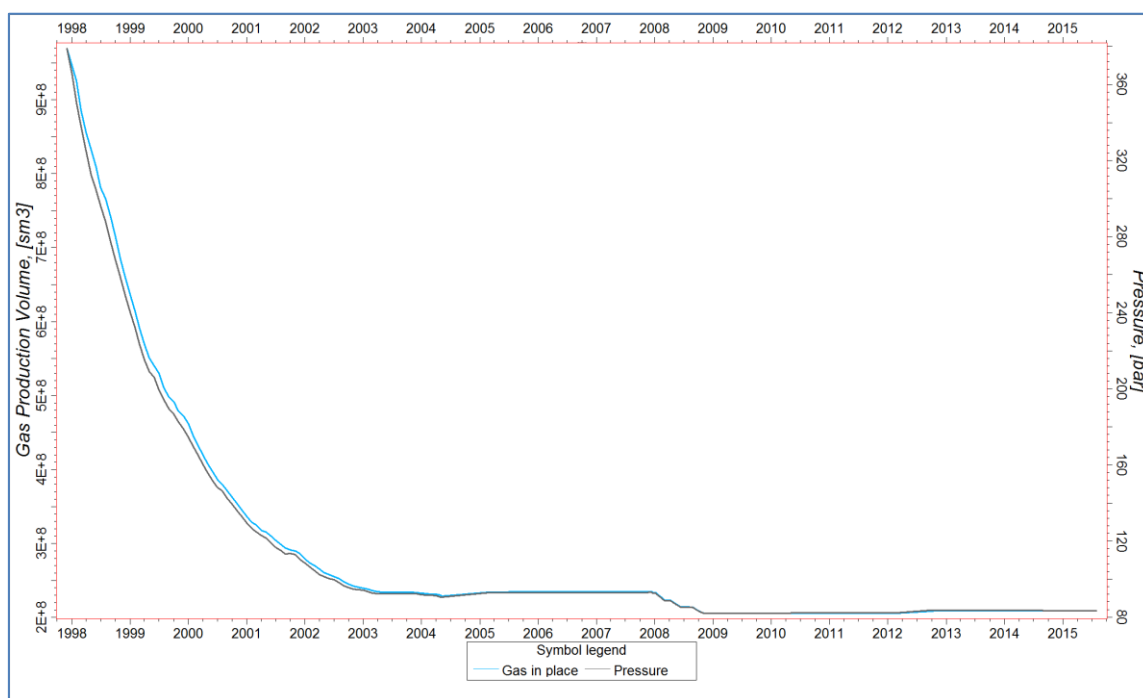


Figure 35: Gas production volume and corresponding reservoir pressure as a function of time.

Figure 35 shows that the gas-initially in place (GIIP) of the simulation is $9.6 \cdot 10^8 \text{ Sm}^3$, which is similar to the estimations of the 8.8 and $9.7 \cdot 10^8 \text{ Sm}^3$ of the GIIP according to the volumetric and material balance calculations, respectively.

Figure 35 shows that the simulated reservoir pressure rises slightly during the suspended state of the well B8 between 2005 and 2008. This rise in pressure can be

attributed to a subdivision of compartment 4. Apparently two sub-compartments exist that are divided by a low transmissivity fault. Due to the fault, a higher pressure was conserved in one sub-compartment that gradually releases its pressure to the main sub-compartment where well B8 is located.

However, a comparison between the simulated and measured CO₂ fractions during first back-production experiments in 2007-2008 shows that simulated values are too high and also provide a different temporal pattern. This means that the actual fate and transport of the CO₂ in the reservoir cannot be fully captured by the simulator.

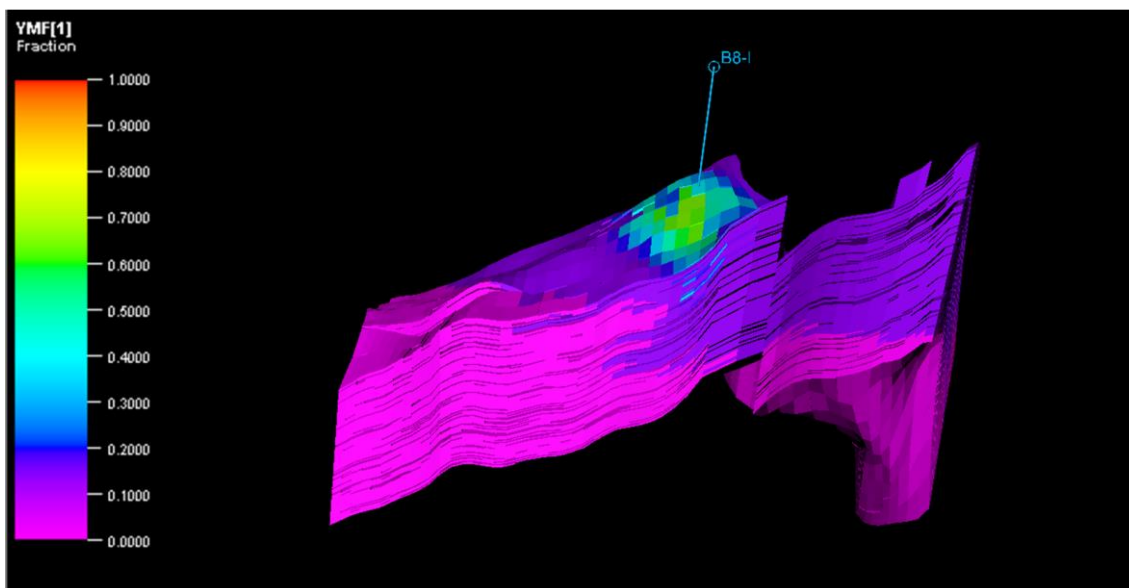


Figure 36: Cross section of molar CO₂ fraction prior to first back-production on November 1st, 2007.

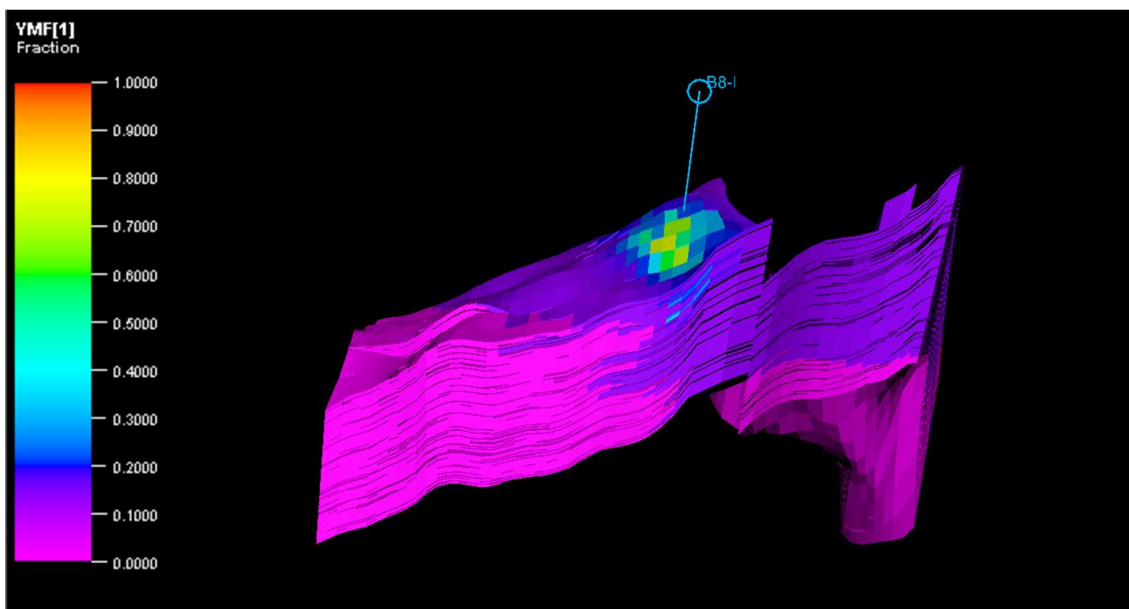


Figure 37: Cross section of molar CO₂ fraction after second back-production period on January 1st, 2015.

The hypothesis of two sub-compartments that are connected by a low transmissivity fault is illustrated in Figure 36 and Figure 37. The injected CO₂ does not spread across the reservoir but stays rather close to the injector (Figure 36, Figure 37). After the second back-production period the molar fractions near the well B8 are even higher in early 2015. This corresponds to the simulation result, that simulated concentrations are higher than observed concentrations at the beginning of both back-production periods. It appears that the back-production pulls the CO₂ closer to the well.

The cumulative injection into the B8 well is 18,710 t, from which 11,974 t was injected before the first back-production test and 6,736 t after the first back-production test

The amount of produced CO₂ was 300 t (along significant amounts of natural gas) during the first test and 20 t (at much higher concentration) during the second test, in 2014. This means that 2.5 % of injected CO₂ was produced in the first test and 0.11 % of injected CO₂ was produced during the second test.

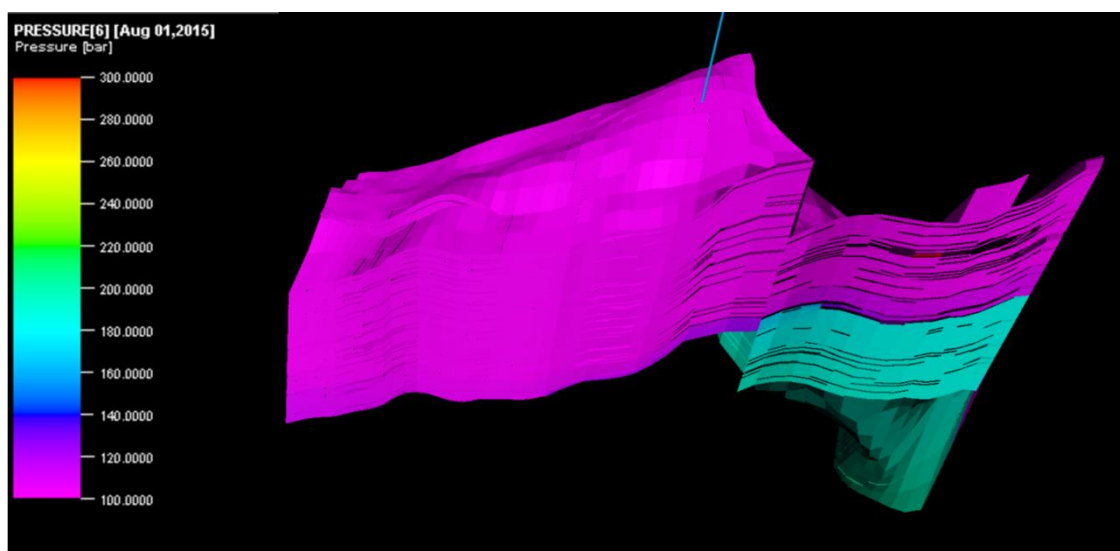


Figure 38: Pressure distribution in the K12-B reservoir at 1 November 2006. Higher pressure in the sub-compartment on the lower right.

Error! Reference source not found. shows the pressure distribution on November 1st 006. At this time the conventional production at the well B8 has ceased. The pressure in the right sub-compartment is higher than that in the left sub-compartment with the well B8. This is due to the low transmissivity of faults between the two sub components. The success during the first back-production can possibly be attributed to a delayed pressure support through fault 2.

Error! Reference source not found. shows that the pressure is almost at equilibrium in 015. This explains the short second re-production period. If the hypothesis of two sub-compartments connected by a low transmissivity fault it true, a third re-production period would also not be successful.

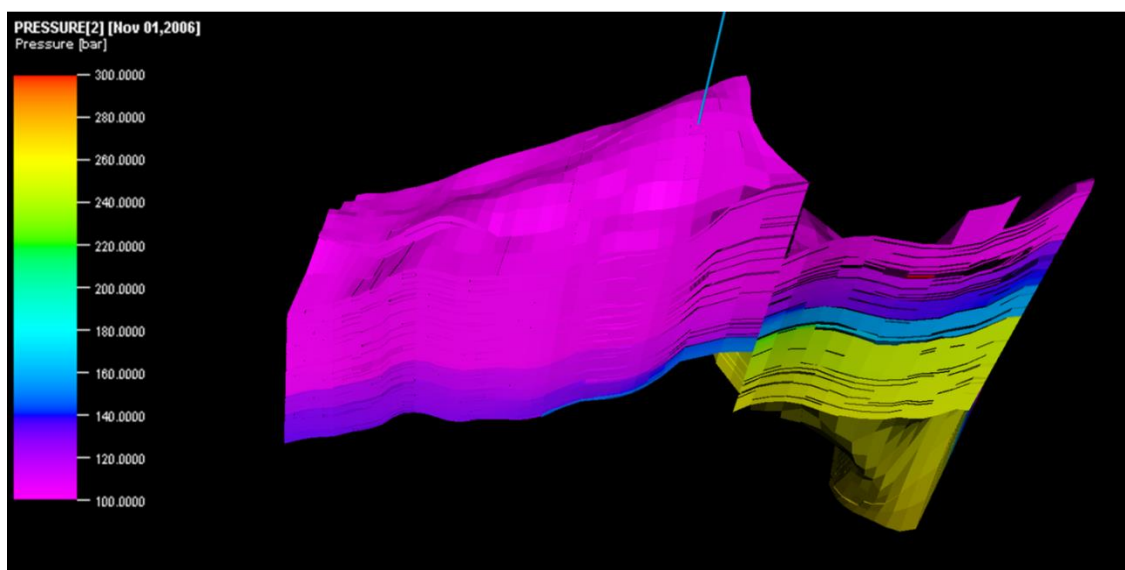


Figure 39: Pressure distribution in the K12-B reservoir at 1 August 2015. Both sub-compartments are near pressure equilibrium.

5.5 Discussion

A compositional model was applied for history matching two back-production experiments at the mature gas field K12-B. Although the predictions are close to the actual measurements, it cannot completely reproduce the measured values as a function of time. A considerable amount of gas could be produced on the first back-production period, only a very small amount was retrieved during the second back-production period. A plausible explanation for this behaviour was found. The reservoir is divided in two sub-compartments that are connected by a low transmissivity fault. After the end of the regular gas production, the second sub-compartment was still pressurized with the consequence of continuous gas flow into the main sub-compartment with the producing well B8. During a further waiting period the overpressure of the small sub-compartment was nearly equilibrated and only very little amount of gas could penetrate into the main sub-compartment. Therefore only a small amount of gas could be retrieved during the second back-production period. A further back-production period does not appear to be successful. The amount of back-produced CO₂ was 2.5 % during the first and around 0.1 % during the second back-production period. As the two tests were ended when the production had ceased, the maximum possible volume of CO₂ was back-produced. The back-production experiments were carried out when the gas reservoir was very mature and reservoir pressure decreased to around 80 bar. The back-production rates can be expected to be higher when the gas reservoir filled until values close or equal to the initial reservoir pressure (around 380 bar), commonly used for CCS projects.

6 SUMMARY

The field experiment at the Ketzin pilot site has shown that a safe back-production of CO₂ is generally feasible, and can be performed at both stable reservoir and wellbore conditions. The official permission document by the Mining Authority of the Federal State of Brandenburg for starting the experiment, and a brief summary of key operational data were provided as Milestones 10 and 11. The recorded pressure and temperature data were released to the modelling groups.

Over the entire test period, the back-production of CO₂ at the pilot site Ketzin ran stable and reliable regarding the CO₂ production rates and the corresponding pressure values above and below ground. There were no work accidents or environmental-related events.

From October 15 to 27, 2015, approximately 240 tonnes of CO₂ and around 62 tonnes of deposit water were produced from the wellbore Ktzi 201. The extracted gas consisted of > 97% of CO₂. As second most component nitrogen was observed. The gas was released by a stack system in the ambient air. The co-produced high-saline formation water has been disposed as waste.

The back-production experiment at Ketzin shows that the reservoir pressure can be effectively lowered by the back-production of CO₂. However, the pressure level reestablishes rapidly after the back-production is stopped. No permanent reduction of the reservoir pressure could be observed. Even at low rates significant amounts of brine are produced at a much higher rate than previously expected. Hence, its disposal requires additional effort. In conclusion, it can be said that back-production of small amounts is feasible as a temporal remediation measure.

The reservoir model developed for the Ketzin field was history-matched using the bottomhole pressure data recorded during the CO₂ back-production experiment. Scenarios considering back-production for an extended period were also simulated assuming both constant and variable production rates in order to understand the associated reservoir pressure behaviour. The simulated bottomhole pressures at the well Ktzi 201 indicate that the decrease in pressure would potentially range between 10-40 bars if the back-production is sustained for a period of four months.

A near wellbore geomechanical model based on Ketzin field has been developed. The whole cycle of well drilling, completion, CO₂ injection and back-production was simulated. It has been found that the pressure increase induced by CO₂ injection can marginally enlarge the failure zone around the wellbore. On the other hand, decreasing the near wellbore pore pressure has almost no effect on the failure zone developed earlier, and its size remains the same after CO₂ back-production.

For the K12-B gas field as a real-production case study, two back-production periods have been investigated. Although the numerical predictions are close to the actual measurements, they cannot completely reproduce the measured values of gas and water production as a function of time. The given structure of the reservoir (compartments with different pressure levels, low transmissivity faults) constitute challenging constraints for the applied compositional reservoir simulator. Further numerical studies needs to be applied here.

7 REFERENCES

- BGS, 2008. A joint research project report on “Reactions between CO₂ and borehole infrastructure” by British Geological Survey, Imperial College, IFP Energies Nouvelles and Bureau de Recherches Géologiques et Minières (2008): Report submitted to European Commission during the CO₂GeoNet project.
- Birkholzer, J. T., Zhou, Q., and Tsang, C.-F., 2009. Large-scale impact of CO₂ storage in deep saline aquifers: A sensitivity study in pressure response in stratified systems. *International Journal of Greenhouse Gas Control* 3, 181-194.
- Celia, M.A., Bachu, S., Nordbotten, J. M., Gasda, S.E. and Dahle, H.K. (2005): Quantitative Estimation of CO₂ Leakage from Geological Storage: Analytical Models, Numerical Models and Data Needs. In Rubin, E.S., Keith, D.W. and Gilboy C.F. (eds.) *Proceedings of 7th International Conference on Greenhouse Gas Control Technologies (GHGT-7)*. September 5-9, 2004, Vancouver, Canada, v.I, 663–672
- Chen, F., Wiese, B., Zhou, Q., Kowalsky, M., Norden, B., Kempka, T., Birkholzer, J. (2014): Numerical modeling of the pumping tests at the Ketzin pilot site for CO₂ injection: Model calibration and heterogeneity effects, *International Journal of Greenhouse Gas Control* 22, 200-212.
- Class, H., Mahl, L., Ahmed, W., Norden, B., Kühn, M., Kempka, T. (2015): Matching pressure measurements and observed CO₂ arrival times with static and dynamic modelling at the Ketzin storage site. *European Geosciences Union General Assembly 2015, EGU, Division Energy, Resources & Environment, ERE, Energy Procedia* 76, 623 - 632, doi: 10.1016/j.egypro.2015.07.883.
- Grond, L. and Holstein, J. (2014): Power-to-gas: Climbing the technology readiness ladder. *Gas for Energy* 2, 20-25.
- James, R. (2013): Novel CO₂ Utilization Concepts: Working Paper. US Department of Energy DOE/NETL-2012/1588.
- Kempka, T., Kühn, M. (2013): Numerical simulations of CO₂ arrival times and reservoir pressure coincide with observations from the Ketzin pilot site, Germany, *Environmental Earth Sciences*, 70 (8), 3675-3685.
- Kempka, T., Class, H., Görke, U.-J., Norden, B., Kolditz, O., Kühn, M., Walter, L., Wang, W., Zehner, B. (2013): A Dynamic Flow Simulation Code Intercomparison based on the Revised Static Model of the Ketzin Pilot Site. *Energy Procedia*, Volume 40, Pages 418-427, doi:10.1016/j.egypro.2013.08.048.
- Manceau, J.-C., Hatzignatiou, D. G., de Lary, L., Jensen, N. B., Réveillère, A. (2014): Mitigation and remediation technologies and practices in case of undesired migration of CO₂ from a geological storage unit - Current status. *International Journal of Greenhouse Gas Control* 22, 272–290. doi: 10.1016/j.ijggc.2014.01.007
- Martens, S., Kempka, T., Liebscher, A., Möller, F., Schmidt-Hattenberger, C., Streibel, M., Szizybalski, A., Zimmer, M. (2015): Field experiment on CO₂ back-production at the Ketzin pilot site. *European Geosciences Union General Assembly 2015, EGU, Division Energy, Resources & Environment, ERE, Energy Procedia* 76 (2015) 519 - 527, doi: 10.1016/j.egypro.2015.07.902.
- Neele, F., Quinquis, H., Read, A., Wright, M., Lorsong, J., Poulussen, D. F., 2014. CO₂

storage development: Status of the large European CCS projects with EPR funding. *Energy Procedia* 63, 6053-6066.

Nordbotten, J.M., Celia, M.A., Bachu, S., Dahle, H.K. (2005): Semi-analytical Solution for CO₂ Leakage through an Abandoned Well, *Environ. Sci. Technol.* 39, 602-611.

Norden, B. & Frykman, P. (2013): Geological modelling of the Triassic Stuttgart Formation at the Ketzin CO₂ storage site, Germany, *International Journal of Greenhouse Gas Control* 19, 756-774.

Panin, G.N. and Brezgunov, V.S. (2006): Influence of the salinity of water on its evaporation. *Atmospheric and Oceanic science* 43-663-665.

Pruess, K. (2006): On CO₂ Behaviour in the Subsurface, Following Leakage from a Geologic Storage Reservoir. Lawrence Berkeley National Laboratory, 12.PROCEEDINGS, CO₂SC Symposium Lawrence Berkeley National Laboratory, Berkeley, California, March 20-22, 2006, 178-181. www.osti.gov/scitech/servlets/purl/881621

Pruess, K. (2008): Leakage of CO₂ from geologic storage: Role of secondary accumulation at shallow depth. *International Journal of Greenhouse Gas Control* 2, 37-46.

Schlumberger. Eclipse Technical Manual 2009.

Vandeweyer, V. P., Van der Meer, L. G. H, Hofstee, C. (2008): Monk Monitoring K12-B. TNO Report 2008-U-R1329/B

Vandeweyer, V. P., Van der Meer, L.G.H, Hofstee, C., Mulders, F. M. M, D'Hoore, D., Graven, H. (2011): Monitoring the CO₂ injection site: K12-B. *Energie Procedia* 4, 5471-5478.

Van der Meer, L. G. H, Kreft, E and Geel, C. R. (2005): K12-B: A test site for CO₂ storage and enhanced gas recovery. *SPE* 94128.

Van der Meer, L. G. H., Arts, R. J., Geel, C. R., Hofstee, C., Winthagen, P., Hartman, J., D'Hoore, D. (2009), K12-B: Carbon dioxide injection in a nearly depleted gas field offshore the Netherlands, in M. Grobe, J. C. Pashin, and R. L. Dodge, eds., *Carbon dioxide sequestration in geological media—State of the science: AAPG Studies in Geology* 59, p. 379–390.

Yamamoto H., Zhang K., Karasaki K., Marui A., Uehara H. and Nishikawa N. (2009): Numerical investigation concerning the impact of geologic storage on regional groundwater flow. *International Journal of Greenhouse Gas Control* 3, 586-599.